Electronic Supplementary Information

The acid-mediated isomerization of iridium(III) complexes with cyclometalated NHC ligands: kinetic *vs* thermodynamic control

*Anastasia Yu. Gitlina, Farzaneh Fadaei-Tirani, and Kay Severin**

Institut des Sciences et Ingénierie Chimiques, École Polytechnique Fédérale de Lausanne (EPFL), 1015 Lausanne, Switzerland

Table of contents

Materials and methods

Unless otherwise stated, all chemical reactions were carried out under an atmosphere of dry N_2 using Schlenk or Glovebox techniques. All reagents and solvents were purchased from chemical suppliers (Precious Metals Online, Sigma Aldrich, Fluorochem, TCI, Apollo) and used as received. Dry solvents were obtained from a solvent purification system with activated aluminum oxide columns (Innovative Technology, Inc.).

All NMR scale experiments were provided under the inert atmosphere of dry N_2 inside a Glovebox (MBraun). Stock solutions of trifluoroacetic acid (TFA, 0.5 M), bistriflimidic acid ($HNTf_2$, 0.2 M), and triethylamine (NEt_3, 0.5 M) were prepared in CD_2Cl_2 passed through the basic alumina column prior the experiments.

Flash column chromatography was performed using silica gel 230–400 mesh (Silicycle, Inc.) and MP alumina (Brockmann activity II–III, EcoChrom^{TM}).

Solution ^1H, ^{13}C {^1H}, ^{19}F {^1H}, ^1H–^1H COSY and ^1H–^{13}C HSQC NMR spectra were recorded at indicated temperatures on a Bruker Avance 400 MHz and on a Bruker Avance Neo 500 MHz spectrometers. All chemical shifts (δ) are reported in ppm and aligned with respect to the residual signal of corresponding deuterated solvent.[1]

Nanochip-based electrospray ionization (ESI) high resolution mass spectrometry (HRMS) was provided on a Linear Trap Quadrupole (LTQ) Orbitrap Elite ETD spectrometer (Thermo Fisher) operated in positive mode.

Synthesis of the facial isomers of $Ir(pmb)_3$, $Ir(pbb)_3$ and $Ir(tzp)_3$

Facial isomers of complexes $Ir(pmb)_3$ and $Ir(pbb)_3$, where pmb is cyclometalated 1-phenyl-3-methylbenzimidazolin-2-ylidene and pbb is 1-phenyl-3-benzylbenzimidazolin-2-ylidene, were prepared following the procedure described by Johannes and co-workers with slightly modified conditions (Scheme S1).[2]

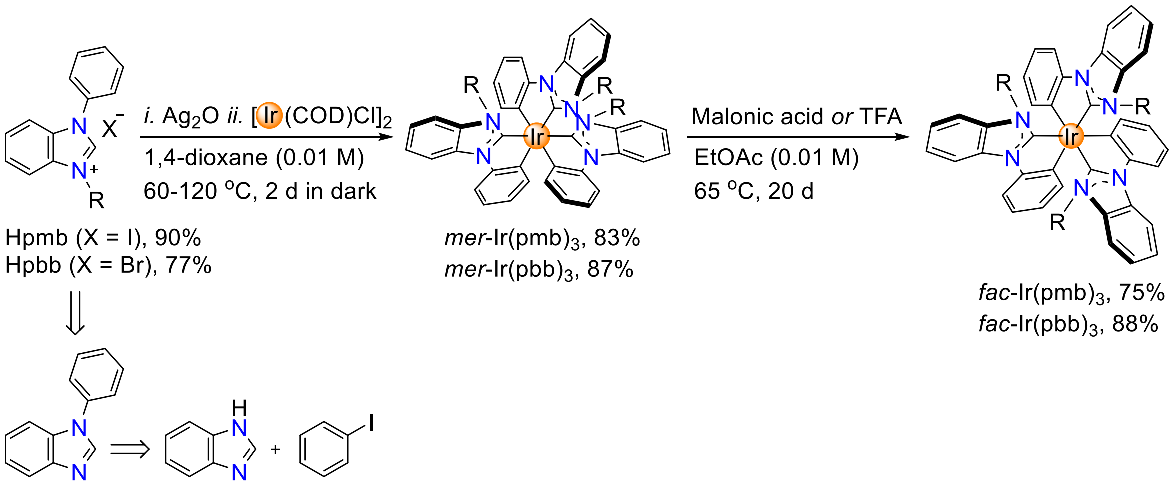

Scheme S1. Synthesis of the *fac* isomers of $Ir(pmb)_3$ and $Ir(pbb)_3$.

***mer*-Ir(pmb)₃**. Obtained from $[Ir(COD)Cl]_2$ (750 mg, 1.12 mmol, 1 eq.), Ag_2O (1.29 g, 5.58 mmol, 5 eq.) and Hpmbi (3.75 g, 11.2 mmol, 10 eq.). White powder, 1.51 g (83%). **^{1}H NMR** (400 MHz, CD_2Cl_2, 298 K) δ 8.19 (t, J = 8.5 Hz, 2H), 8.12 (d, J = 8.1 Hz, 1H), 7.89 (dd, J = 7.4, 1.9 Hz, 2H), 7.84 (d, J = 8.0 Hz, 1H), 7.39 – 7.21 (m, 9H), 7.06 – 6.96 (m, 3H), 6.86 (dt, J = 7.1, 1.7 Hz, 2H), 6.70 – 6.58 (m, 4H), 3.31 (s, 3H), 3.26 (s, 3H), 3.20 (s, 3H). **^{13}C {^{1}H} NMR** (101 MHz, CD_2Cl_2, 298 K) δ 188.9, 186.3, 185.3, 151.7, 150.3, 150.1, 149.4, 148.4, 148.0, 139.4, 139.2, 137.2, 137.2, 136.7, 133.0, 132.9, 125.2, 124.9, 124.6, 123.1, 123.1, 122.4, 122.3, 122.2, 121.2, 120.8, 120.8, 113.0, 112.9, 112.5, 111.6, 111.5, 110.2, 110.2, 110.2, 33.8, 33.7, 33.2.

***mer*-Ir(pbb)₃**. Obtained from $[Ir(COD)Cl]_2$ (243 mg, 0.36 mmol, 1 eq.), Ag_2O (419 mg, 1.81 mmol, 5 eq.) and Hpmbi (1.32 g, 3.62 mmol, 10 eq.). White powder, 656 mg (87%). **^{1}H NMR** (400 MHz, CD_2Cl_2, 298 K) δ 8.17 (d, J = 8.4 Hz, 1H), 7.89 (d, J = 7.8 Hz, 1H), 7.84 – 7.77 (m, 1H), 7.48 – 7.39 (m, 2H), 7.31 (ddd, J = 8.4, 7.3, 1.2 Hz, 1H), 7.23 (ddd, J = 8.4, 7.3, 1.3 Hz, 1H), 7.19 (d, J = 7.9 Hz, 1H), 7.14 (tdd, J = 7.3, 2.8, 0.9 Hz, 2H), 7.10 – 7.00 (m, 5H), 6.96 (dd, J = 7.1, 1.5 Hz, 1H), 6.93 – 6.74 (m, 9H), 6.72 – 6.58 (m, 8H), 6.38 – 6.32 (m, 2H), 6.24 (dd, J = 11.8, 8.3 Hz, 4H), 5.54 – 5.33 (m, 3H), 5.03 (d, J = 16.7 Hz, 1H), 4.93 (d, J = 16.2 Hz, 1H), 4.69 (d, J = 16.3 Hz, 1H). **^{13}C {^{1}H} NMR** (101 MHz, CD_2Cl_2, 298 K) δ 190.3, 185.8, 185.6, 151.6, 150.3, 149.2, 148.5, 146.7, 139.1, 138.3, 137.3, 136.8, 136.7, 136.5, 136.3, 136.2, 135.3, 133.3, 133.2, 132.9, 128.3, 128.0, 128.0, 127.2, 126.9, 125.9, 125.6, 125.4, 125.2, 124.9, 124.5, 123.3, 123.1, 122.6, 122.4, 122.3, 122.0, 121.1, 120.9, 120.7, 113.5, 113.3, 113.0, 112.1, 112.1, 111.8, 110.9, 110.8, 110.4, 51.0, 50.9, 50.8.

***fac*-Ir(pmb)$_3$**. Obtained by malonic acid-mediated (MA, 1 M in deionized water, 5.30 mL, 10 eq.) isomerization of *mer*-Ir(pmb)$_3$ (433 mg, 0.53 mmol, 1.00 eq.) with a reaction time of 20 d. White powder, 325 mg (75%). **^{1}H NMR** (400 MHz, CD_2Cl_2, 298 K) δ 8.15 (dt, *J* = 8.3, 0.9 Hz, 1H), 7.87 (dd, *J* = 8.0, 1.1 Hz, 1H), 7.35 – 7.29 (m, 1H), 7.28 – 7.18 (m, 2H), 7.03 (ddd, *J* = 7.9, 7.3, 1.6 Hz, 1H), 6.65 (td, *J* = 7.3, 1.1 Hz, 1H), 6.55 (dd, *J* = 7.2, 1.6 Hz, 1H), 3.28 (s, 3H). **^{13}C {^{1}H} NMR** (126 MHz, CD_2Cl_2, 298 K) δ 190.1, 149.3, 148.9, 137.0, 136.7, 133.0, 124.7, 123.1, 122.2, 121.4, 112.5, 111.5, 110.2, 33.9.

***fac*-Ir(pbb)$_3$**. Obtained by trifluoroacetic acid-mediated (TFA, 1 M in deionized water, 5.00 mL, 10 eq.) isomerization of *mer*-Ir(pbb)$_3$ (521 mg, 0.50 mmol, 1 eq.) with a reaction time of 20 d. White powder, 458 mg (88%). **^{1}H NMR** (400 MHz, CD_2Cl_2, 298 K) δ 7.78 (d, *J* = 8.3 Hz, 1H), 7.61 (d, *J* = 8.0 Hz, 1H), 7.13 (ddd, *J* = 8.4, 7.3, 1.2 Hz, 1H), 7.05 – 7.00 (m, 2H), 6.99 – 6.94 (m, 1H), 6.88 (d, *J* = 8.0 Hz, 1H), 6.83 – 6.75 (m, 2H), 6.66 (td, *J* = 7.3, 1.1 Hz, 1H), 6.55 (dd, *J* = 7.3, 1.6 Hz, 1H), 6.21 – 6.13 (m, 2H), 5.27 (d, *J* = 16.4 Hz, 1H), 4.82 (d, *J* = 16.4 Hz, 1H). **^{13}C {^{1}H} NMR** (126 MHz, CD_2Cl_2, 298 K) δ 190.6, 149.5, 148.7, 136.5, 135.9, 135.2, 133.1, 128.4, 127.3, 125.5, 125.2, 124.6, 122.9, 122.1, 121.3, 113.1, 111.7, 110.4, 51.7.

The NMR spectra of *fac* and *mer* isomers of Ir(pmb)$_3$ and Ir(pbb)$_3$ are in agreement with those reported in the literature.[2]

The *fac* isomer of complex Ir(tzp)$_3$, where tzp is cyclometalated 1-phenyl-1,2,4-triazolo[4,3-*f*]phenanthridilin-2-ylidene, was prepared following the procedure described by Kang and co-workers with slightly modified conditions (Scheme S2).[3] The precursor for the cyclometalated carbene ligand was obtained in two steps from 9-fluorenone.[4]

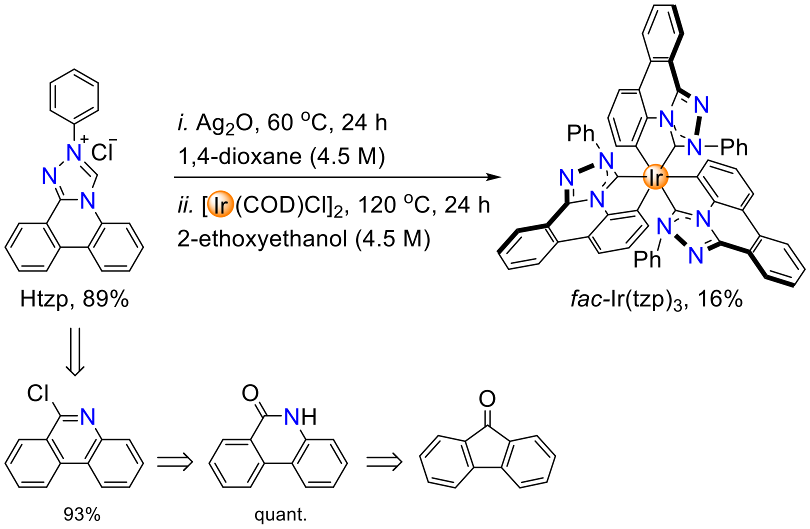

Scheme S2. Synthesis of *fac*-Ir(tzp)$_3$.

***fac*-Ir(tzp)$_3$**. Obtained from [Ir(COD)Cl]$_2$ (2.84 g, 4.22 mmol, 1 equiv.), Ag$_2$O (4.89 g, 21.1 mmol, 5 equiv.) and Htzp (14.0 g, 42.2 mmol, 10 equiv.). Cream-colored powder, 1.45 g (16%). **^{1}H NMR** (400 MHz, CD_2Cl_2, 298 K) δ 8.48 (d, *J* = 8.0 Hz, 1H), 8.35 (dd, *J* = 8.0, 1.3 Hz, 1H), 7.87 (dd, *J* = 8.1, 1.0 Hz, 1H), 7.79 (ddd, *J* = 8.4, 7.2, 1.4 Hz, 1H), 7.63 (ddd, *J* = 8.1, 7.2, 1.1 Hz, 1H), 7.26 (tt, *J* = 7.5, 1.2 Hz, 1H), 7.11 (dd, *J* = 8.0, 7.2 Hz, 1H), 6.99 – 6.81 (m, 3H), 6.24 – 6.07 (m, 2H). **^{13}C {^{1}H} NMR** (101 MHz, CD_2Cl_2, 298 K) δ 169.0, 146.4, 144.4, 140.3, 139.8, 138.2, 134.4, 131.4, 128.7, 128.7, 128.1, 127.0, 125.4, 125.2, 124.5, 119.6, 118.9, 115.7.

General procedure for the $HNTf_2$–NEt_3 *fac→mer* isomerization

The general procedure for the $HNTf_2$–NEt_3-induced *fac→mer* isomerization of Ir(C^C:)$_3$ complexes (C^C: = pmb, pbb) is shown in the Scheme S3.

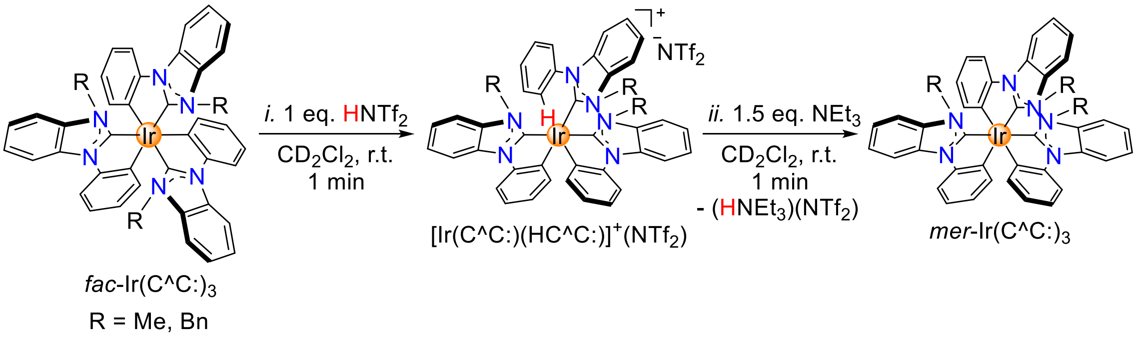

Scheme S3. The *fac→mer* isomerization of Ir(C^C:)$_3$ complexes.

The *fac* isomer of the respective Ir(C^C:)$_3$ complex (1 eq.) was placed in a 5 mL vial equipped with a stirring bar and dissolved in 0.5 mL of CD_2Cl_2 resulting in a colorless solution. Subsequently, a stock solution of $HNTf_2$ (0.2 M in CD_2Cl_2, 1 eq.) was added in one portion under vigorous stirring (1100 rpm). The reaction was accompanied by a change of color to yellow. After 1 min of stirring at RT, the solution was transferred to an NMR tube, and a spectrum of the protonated complex [Ir(C^C:)$_2$(HC^C:)](NTf_2) was recorded. Then, the solution of [Ir(C^C:)$_2$(HC^C:)](NTf_2) was transferred back to the vial, and a stock solution of NEt_3 (0.5 M in CD_2Cl_2, 1.5 equiv.) was added slowly dropwise under vigorous stirring (1100 rpm). The reaction was accompanied by a change of solution color back to colorless. After 1 min of stirring at RT, the solution was transferred to an NMR tube, and a spectrum of *mer*-Ir(C^C:)$_3$ was recorded.

Additionally, ^1H, ^{19}F {^1H} and ^{13}C {^1H} NMR spectra of $HNTf_2$ in CD_2Cl_2 were recorded to distinguish the signals of counter anion NTf_2 in ^{13}C spectra of [Ir(C^C:)$_2$(HC^C:)](NTf_2) complexes and follow the shifts in ^1H and ^{19}F spectra.

$HNTf_2$. **^1H NMR** (400 MHz, CD_2Cl_2, 298 K) δ 8.03 (s). **^{19}F {^1H} NMR** (376 MHz, CD_2Cl_2, 298 K) δ –75.3 (s). **^{13}C {^1H} NMR** (101 MHz, CD_2Cl_2, 298 K) δ 119.1 (q, *J* = 322.1 Hz).

[Ir(pmb)$_2$(Hpmb)](NTf_2). A solution of the protonated complex was obtained by the addition of a stock solution of $HNTf_2$ (0.2 M in CD_2Cl_2, 91.3 μL, 18.3 μmol, 1 equiv.) to a solution of *fac*-Ir(pmb)$_3$ (14.9 mg, 18.3 μmol, 1 equiv.) in 0.5 mL of CD_2Cl_2. **^1H NMR** (500 MHz, CD_2Cl_2, 298 K) δ 8.34 – 8.26 (m, 1H), 8.10 (d, *J* = 8.2 Hz, 1H), 8.03 (d, *J* = 7.6 Hz, 1H), 7.91 (dd, *J* = 7.9, 1.3 Hz, 1H), 7.83 (dd, *J* = 8.1, 1.1 Hz, 1H), 7.67 (m, 1H), 7.60 – 7.34 (m, 10H), 7.17 – 7.07 (m, 3H), 6.79 (td, *J* = 7.4, 1.0 Hz, 1H), 6.59 (td, *J* = 7.6, 1.3 Hz, 1H), 6.55 (dd, *J* = 7.2, 1.4 Hz, 1H), 6.24 (dd, *J* = 7.8, 1.3 Hz, 1H), 6.06 (broad s, 2H), 3.91 (s, 3H), 3.27 (s, 3H), 3.10 (s, 3H). **^{19}F {^1H} NMR** (471 MHz, CD_2Cl_2, 298 K) δ –79.5 (s). **^{13}C {^1H} NMR** (126 MHz, CD_2Cl_2, 298 K) δ 183.4 (s), 182.9 (s), 179.5 (s), 149.6 (s), 146.7 (s), 144.9 (s), 139.1 (s), 137.8 (s), 136.5 (s), 136.2 (s), 135.9 (s), 135.6 (s), 134.5 (s), 132.5 (s), 131.9 (s), 131.8 (s), 129.4 (s), 126.4 (s), 125.8 (s), 125.5 (s), 125.5 (s), 125.3 (s), 125.2 (s), 125.0 (s), 124.6 (s), 124.2 (s), 123.9 (s), 123.7 (s), 120.3 (q, *J* = 321.8 Hz), 114.8 (s), 113.8 (s), 112.6 (s), 112.5 (s), 112.4 (s), 111.8

(s), 111.8 (s), 111.8 (s), 35.0 (s), 33.8 (s), 33.0 (s). **HRMS** (nanochip-ESI/LTQ-Orbitrap) m/z: $[M]^+$ calcd. for $C_{42}H_{34}IrN_6^+$ 815.2469; found 815.2449.

***mer*-Ir(pmb)$_3$**. A solution of the *mer* isomer was obtained by the addition of a stock solution of NEt_3 (0.5 M in CD_2Cl_2, 54.8 µL, 27.4 µmol, 1.5 equiv.) to the solution of [Ir(pmb)$_2$(Hpmb)](NTf$_2$). The ^{1}H NMR spectrum of *mer*-Ir(pmb)$_3$ obtained *in situ* is in agreement with the one obtained by conventional synthesis (see Page S3).

[Ir(pbb)$_2$(Hpbb)](NTf$_2$). A solution of the protonated complex was obtained by the addition of a stock solution of HNTf$_2$ (0.2 M in CD_2Cl_2, 53.7 µL, 10.7 µmol, 1 eqiuv.) to a solution of *fac*-Ir(pbb)$_3$ (11.2 mg, 10.7 µmol, 1 equiv.) in 0.5 mL of CD_2Cl_2. **^{1}H NMR** (500 MHz, CD_2Cl_2, 298 K) δ 8.18 (dd, J = 15.3, 8.4 Hz, 1H), 7.87 – 7.59 (m, 3H), 7.51 – 7.27 (m, 9H), 7.22 – 6.71 (m, 17H), 6.68 – 6.35 (m, 5H), 6.26 – 6.13 (m, 4H), 5.36 (d, J = 2.7 Hz, 1H), 5.29 – 5.17 (m, 2H), 5.13 – 4.94 (m, 2H), 4.88 – 4.80 (m, 1H), 4.74 – 4.42 (m, 1H). **^{19}F {^{1}H} NMR** (376 MHz, CD_2Cl_2, 273 K) δ –79.5 (s). **^{13}C {^{1}H} NMR** (126 MHz, CD_2Cl_2, 273 K) δ 183.7, 181.1, 179.1, 149.0, 147.7, 146.7, 146.6, 145.4, 145.1, 144.4, 139.0, 136.7, 135.9, 135.7, 135.5, 135.3, 135.2, 134.5, 134.5, 134.3, 133.8, 133.6, 133.5, 133.5, 132.0, 131.9, 131.0, 129.1, 128.8, 128.7, 128.5, 128.4, 128.1, 128.0, 127.9, 127.5, 127.1, 126.1, 126.1, 125.8, 125.3, 125.3, 125.2, 125.2, 125.1, 125.0, 124.9, 124.8, 124.6, 124.5, 124.4, 124.2, 124.1, 123.3, 121.1, 118.5, 115.2, 114.8, 113.9, 113.5, 112.7, 112.7, 112.5, 111.9, 111.7, 111.6, 111.3, 51.4, 51.2, 49.7. **HRMS** (nanochip-ESI/LTQ-Orbitrap) m/z: $[M]^+$ calcd. for $C_{60}H_{46}IrN_6^+$ 1043.3408; found 1043.3388. Single crystals of [Ir(pbb)$_2$(Hpbb)](NTf$_2$) were obtained by slow gas phase diffusion of pentane into a solution of the mixture of *fac*-Ir(pbb)$_3$ (40.0 mg, 1 eq.) and HNTf$_2$ (10.8 mg, 1 eq.) in dichloromethane at room temperature.

***mer*-Ir(pbb)$_3$**. A solution of the *mer* isomer was obtained by addition of a stock solution of NEt_3 (0.5 M in CD_2Cl_2, 60.3 µL, 30.1 µmol, 10.5 equiv.) to a solution of [Ir(pbb)$_2$(Hpbb)](NTf$_2$). The ^{1}H NMR spectrum of *mer*-Ir(pbb)$_3$ obtained by *fac→mer* isomerization is in agreement with the one obtained by conventional synthesis (see Page S3).

NMR control of *fac*→*mer* isomerization

The *fac*→*mer* isomerization of the complexes Ir(pmb)$_3$ and Ir(pbb)$_3$ was monitored by ^{1}H NMR spectra (400 MHz, CD_2Cl_2, 298 K).

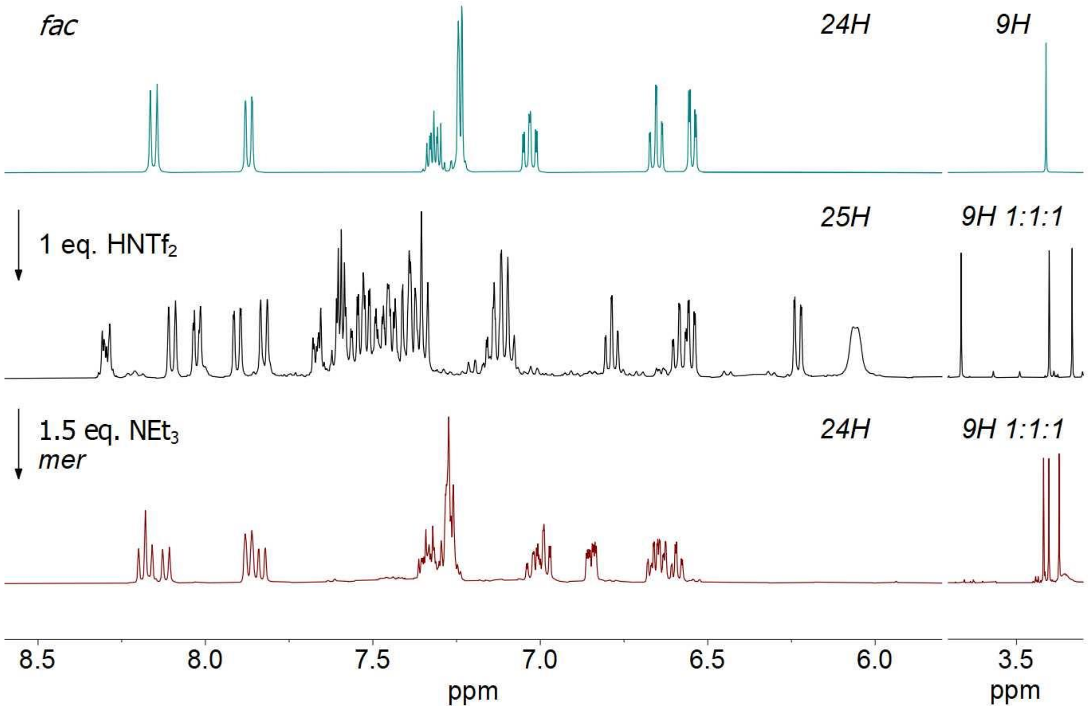

Figure S1. ^{1}H NMR spectra for *fac*→*mer* isomerization for Ir(pmb)$_3$.

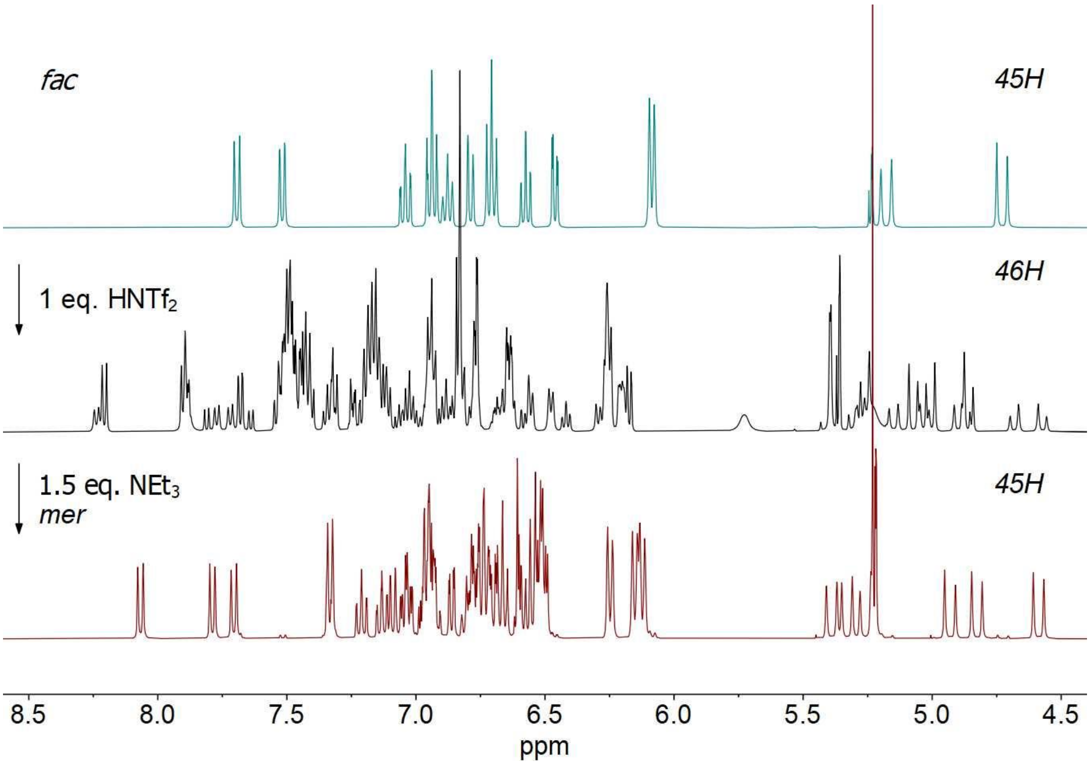

Figure S2. ^{1}H NMR spectra for *fac*→*mer* isomerization for Ir(pbb)$_3$.

TFA–NEt$_3$ treatment of *fac*-Ir(pmb)$_3$

The addition of TFA to *fac*-Ir(pmb)$_3$ (Fig. S3, maroon spectrum) leads to a quantitative conversion to a protonated complex [Ir(pmb)$_3$+TFA] of undefined structure with high symmetry (Fig. S3, black spectrum). The NEt$_3$ treatment of [Ir(pmb)$_3$+TFA] results in a quantitative conversion to a monoprotonated complex of the structure Ir(pmb)$_2$(Hpmb)(CO$_2$CF$_3$) (Fig. S3, yellow spectrum). Further heating of Ir(pmbi)$_2$(Hpmbi)(CO$_2$CF$_3$) at 70 °C overnight gives a mixture of *fac*-Ir(pmb)$_3$ and *mer*-Ir(pmb)$_3$ with the ratio of 1:1.5 (Fig. S3, navy spectrum).

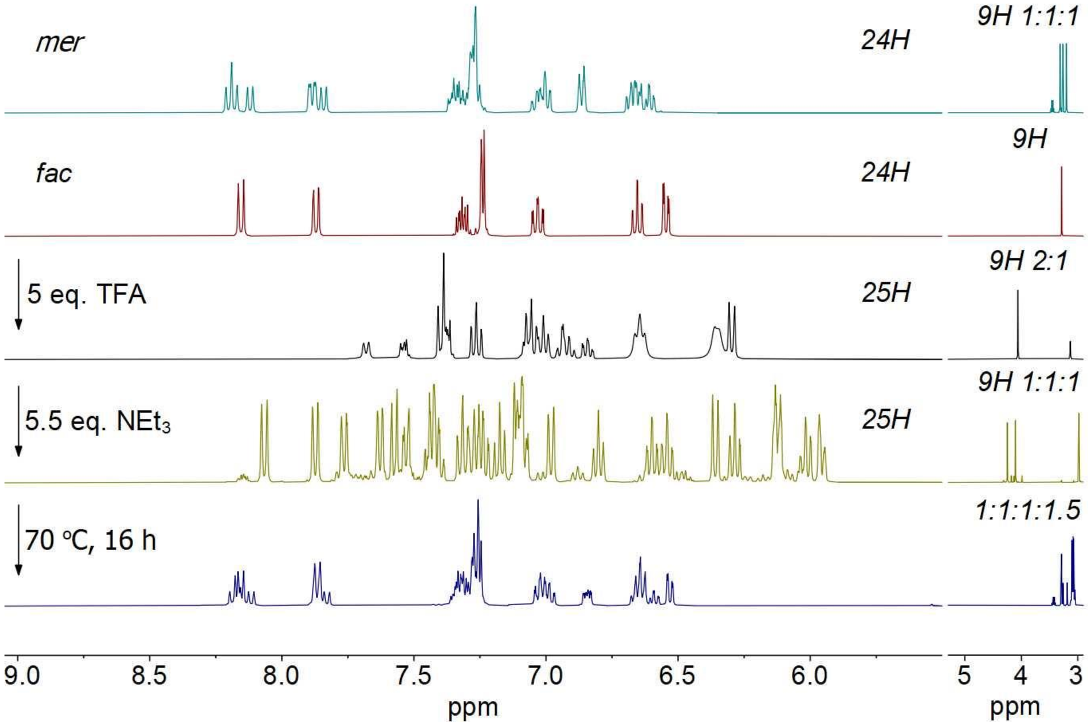

Figure S3. ^{1}H (400 MHz, CD$_2$Cl$_2$) NMR spectra of *mer*-Ir(pmb)$_3$ and the conversion of *fac*-Ir(pmb)$_3$ to a mixture of *fac* and *mer* isomers of Ir(pmb)$_3$.

[Ir(pmb)$_3$+TFA]. *fac*-Ir(pmb)$_3$ (4.16 mg, 5.11 mmol, 1 eq.) was placed in a 5 mL glass vial equipped with a stirring bar and dissolved in 0.5 mL of CD$_2$Cl$_2$ resulting in a colorless solution. Then, a stock solution of TFA (0.5 M in CD$_2$Cl$_2$, 51.1 µL, 25.6 µmol, 5 eq.) was added to the vial in one portion under vigorous stirring (1100 rpm). The reaction was accompanied by a change of color to yellow. After 1 min of stirring at RT, the solution was transferred to an NMR tube, and a spectrum of the protonated complex [Ir(pmb)$_3$+TFA] was recorded. **^{1}H NMR** (400 MHz, CD$_2$Cl$_2$, 298 K) δ 7.68 (d, *J* = 7.6 Hz, 1H), 7.57 – 7.51 (m, 1H), 7.47 – 7.32 (m, 4H), 7.32 – 7.20 (m, 2H), 7.14 – 6.96 (m, 5H), 6.97 – 6.88 (m, 2H), 6.84 (td, *J* = 7.3, 1.8 Hz, 1H), 6.64 (broad t, *J* = 7.7 Hz, 4H), 6.35 (broad d, *J* = 7.7 Hz, 3H), 6.30 (d, *J* = 8.2 Hz, 2H), 4.06 (s, 6H), 3.13 (s, 3H). **HRMS** (nanochip-ESI/LTQ-Orbitrap) m/z: [Ir(pmb)$_3$+H]$^+$ calcd. for $C_{42}H_{34}IrN_6^+$ 815.2469; found 815.2444; [Ir(pmb)$_3$–pmb]$^+$ calcd. for

$C_{28}H_{22}IrN_4^+$ 607.1474; found 607.1451; [Ir(pmb)$_3$+2H]$^{2+}$ calcd. for $C_{42}H_{35}IrN_6^{2+}$ 408.1271; found 408.1259.

Ir(pmb)$_2$(Hpmb)(CO$_2$CF$_3$). The solution of [Ir(pmb)$_3$+TFA] was transferred back to the vial, and a stock solution of NEt$_3$ (0.5 M in CD_2Cl_2, 56.2 µL, 28.1 µmol, 5.5 eq.) was added slowly dropwise under vigorous stirring (1100 rpm). The reaction was accompanied by a change of color back to colorless. After 1 min of stirring at RT, the solution was transferred to an NMR tube, and a spectrum of [Ir(pmb)$_2$(Hpmb)(CO$_2$CF$_3$)] was recorded. **^{1}H NMR** (400 MHz, CD_2Cl_2, 298 K) δ 8.07 (d, *J* = 8.2 Hz, 1H), 7.87 (dd, *J* = 8.0, 1.2 Hz, 1H), 7.78 – 7.74 (m, 1H), 7.63 (dd, *J* = 7.4, 1.6 Hz, 1H), 7.57 (d, *J* = 8.1 Hz, 1H), 7.53 (m, 1H), 7.45 – 7.40 (m, 2H), 7.35 – 7.29 (m, 1H), 7.29 – 7.22 (m, 2H), 7.18 (t, *J* = 7.7 Hz, 1H), 7.13 – 7.05 (m, 3H), 6.98 (dd, *J* = 8.0, 1.3 Hz, 1H), 6.84 – 6.77 (m, 1H), 6.60 (td, *J* = 7.6, 1.5 Hz, 1H), 6.54 (td, *J* = 7.7, 1.5 Hz, 1H), 6.36 (d, *J* = 8.1 Hz, 1H), 6.28 (td, *J* = 7.5, 1.3 Hz, 1H), 6.16 – 6.10 (m, 2H), 6.02 (td, *J* = 7.6, 1.5 Hz, 1H), 5.95 (m, 1H), 4.25 (s, 3H), 4.10 (s, 3H), 2.98 (s, 3H). Single crystals of [Ir(pmb)$_2$(Hpmb)(CO$_2$CF$_3$)] were obtained by slow gas phase diffusion of pentane into a solution of the [Ir(pmb)$_2$(Hpmb)(CO$_2$CF$_3$)] in dichloromethane at RT.

$HNTf_2$–NEt_3 treatment of *fac*-Ir(tzp)$_3$

The addition of $HNTf_2$ to *fac*-Ir(tzp)$_3$ (Fig. S4, teal spectrum) leads to a quantitative conversion to a monoprotonated complex [Ir(tzp)$_2$(Htzp)]$^+$ (Fig. S4, black spectrum). The NEt_3 treatment of [Ir(tzp)$_2$(Htzp)]$^+$ results in a nearly quantitative back-conversion to *fac*-Ir(tzp)$_3$ (Fig. S4, dark teal spectrum).

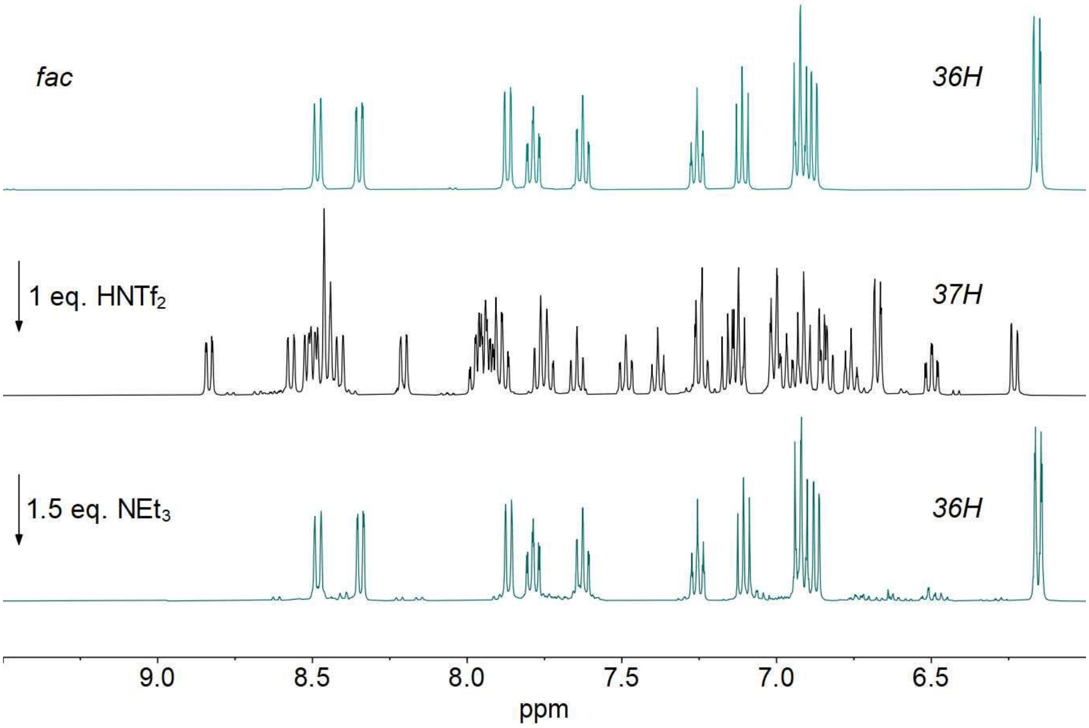

Figure S4. ^1H (400 MHz, CD_2Cl_2) NMR spectra for the conversion of *fac*-Ir(tzp)$_3$ to [Ir(tzp)$_2$(Htzp)]$^+$ by the acid treatment and then back to *fac* by the base addition.

[Ir(tzp)$_2$(Htzp)]$^+$. *fac*-Ir(tzp)$_3$ (16.8 mg, 15.6 μmol, 1 eq.) was placed in a 5 mL glass vial equipped with a stirring bar and dissolved in 0.5 mL of CD_2Cl_2 resulting in a colorless solution. Then, $HNTf_2$ (0.2 M, 78.1 μL, 15.6 μmol, 1 eq.) was added in one portion under vigorous stirring (1100 rpm). The reaction was accompanied by a change of color to yellow. After 1 min of stirring at RT, the solution was transferred to an NMR tube, and a spectrum of the protonated complex [Ir(tzp)$_2$(Htzp)]$^+$ was recorded. **^{1}H NMR** (400 MHz, CD_2Cl_2, 298 K) δ 8.88 – 8.79 (m, 1H), 8.57 (d, *J* = 8.4 Hz, 1H), 8.53 – 8.44 (m, 5H), 8.41 (d, *J* = 8.3 Hz, 1H), 8.21 (dd, *J* = 8.0, 1.3 Hz, 1H), 8.01 – 7.84 (m, 6H), 7.78 – 7.72 (m, 2H), 7.67 – 7.62 (m, 1H), 7.49 (ddd, *J* = 8.3, 7.3, 1.2 Hz, 1H), 7.41 – 7.36 (m, 1H), 7.24 (m, 2H), 7.14 (m, 3H), 7.01 (dd, *J* = 8.6, 1.3 Hz, 2H), 6.99 – 6.95 (m, 1H), 6.93 – 6.89 (m, 2H), 6.87 – 6.81 (m, 2H), 6.79 – 6.73 (m, 1H), 6.69 – 6.65 (m, 2H), 6.50 (td, *J* = 7.7, 1.6 Hz, 1H), 6.23 (dd, *J* = 8.0, 1.1 Hz, 1H). **^{13}C {^{1}H} NMR** (126 MHz, CD_2Cl_2, 260 K) δ 169.6, 164.5, 164.1, 147.7, 147.2, 146.8, 140.5, 140.1, 139.7, 138.0, 137.6, 137.3, 133.1, 132.9, 132.7, 132.6, 132.4, 130.9, 130.6, 130.5, 130.2, 129.5, 129.5, 129.3, 129.2, 129.1, 129.1, 128.8, 128.5, 128.4, 128.3, 127.0, 126.3, 125.4, 125.3, 125.2, 125.1, 124.3, 124.3, 124.0, 123.5, 123.2, 121.2, 119.9, 119.9, 119.7, 118.9, 118.6, 118.5, 118.3, 116.0, 114.5, 110.9. **HRMS**

(nanochip-ESI/LTQ-Orbitrap) m/z: $[M]^+$ calcd. for $C_{60}H_{37}IrN_9^+$ 1076.2796; found 1076.2788. Single crystals of $[Ir(tzp)_2(Htzp)](NTf_2)$ were obtained by slow gas phase diffusion of diethyl ether into a solution of the mixture of *fac*-$Ir(tzp)_3$ (30.6 mg, 1 eq.) and $HNTf_2$ (8.00 mg, 1 eq.) in dichloromethane at room temperature.

Ligand scrambling experiment

An equimolar mixture of *fac*-Ir(pmb)$_3$ and *fac*-Ir(pbb)$_3$ was prepared and treated with first HNTf$_2$ and then NEt$_3$. High-resolution mass spectra recorded before and after isomerization are nearly identical which indicates that ligand scrambling during isomerization is negligible.

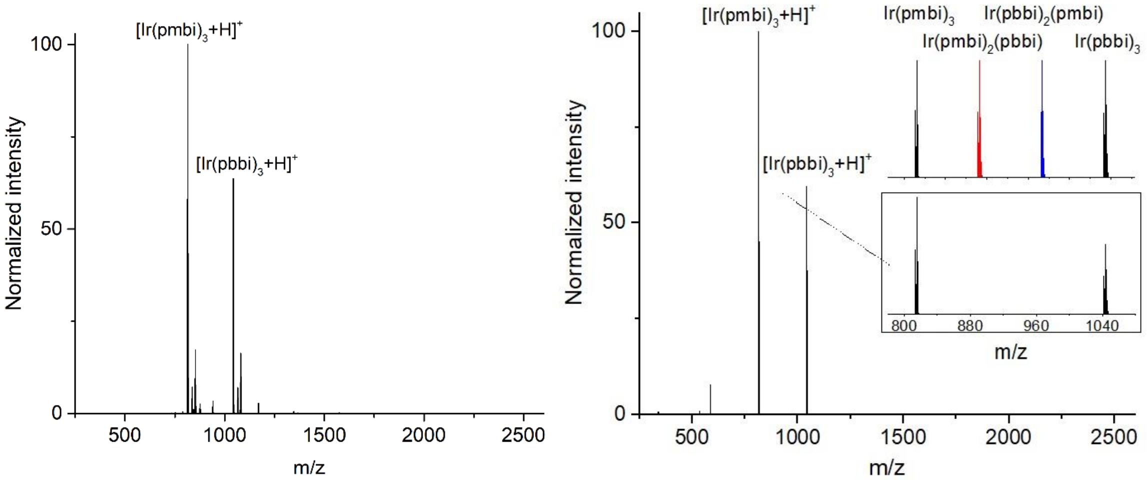

Figure S5. Nanochip-ESI$^+$ HRMS of the starting mixture of *fac*-Ir(pmb)$_3$ and *fac*-Ir(pbb)$_3$ (left) and after its *fac→mer* isomerization (right). Simulated spectra of the hypothetical heteroleptic complexes are shown in color.

Table S1. HRMS data.

Compound	Formula	Calculated [M+H]$^+$, m/z	Found [M+H]$^+$, m/z	
			Before isomerization	*fac→mer*
Ir(pmb)$_3$	$C_{42}H_{33}IrN_6$	815.2469	815.2476	815.2461
Ir(pmb)$_2$(pbb)	$C_{48}H_{37}IrN_6$	891.2784	*not found*	*not found*
Ir(pbb)$_2$(pmb)	$C_{54}H_{41}IrN_6$	967.3097	*not found*	*not found*
Ir(pbb)$_3$	$C_{60}H_{45}IrN_6$	1043.3411	1043.3402	1043.3432

Conversion of the mixture *fac* + *mer* to *mer*

An equimolar mixture of *fac*-Ir(pmb)$_3$ (Fig. S6, teal spectrum) and *mer*-Ir(pmb)$_3$ (Fig. S6, maroon spectrum) was prepared (Fig. S6, navy spectrum). The treatment of the mixture by HNTf$_2$ leads to quantitative conversion to the protonated complex [Ir(pmb)$_2$(Hpmb)]$^+$ (Fig. S6, black spectrum). The NEt$_3$ addition to [Ir(pmb)$_2$(Hpmb)]$^+$ results in a quantitative conversion to *mer*-Ir(pmb)$_3$ (Fig. S6, dark maroon spectrum).

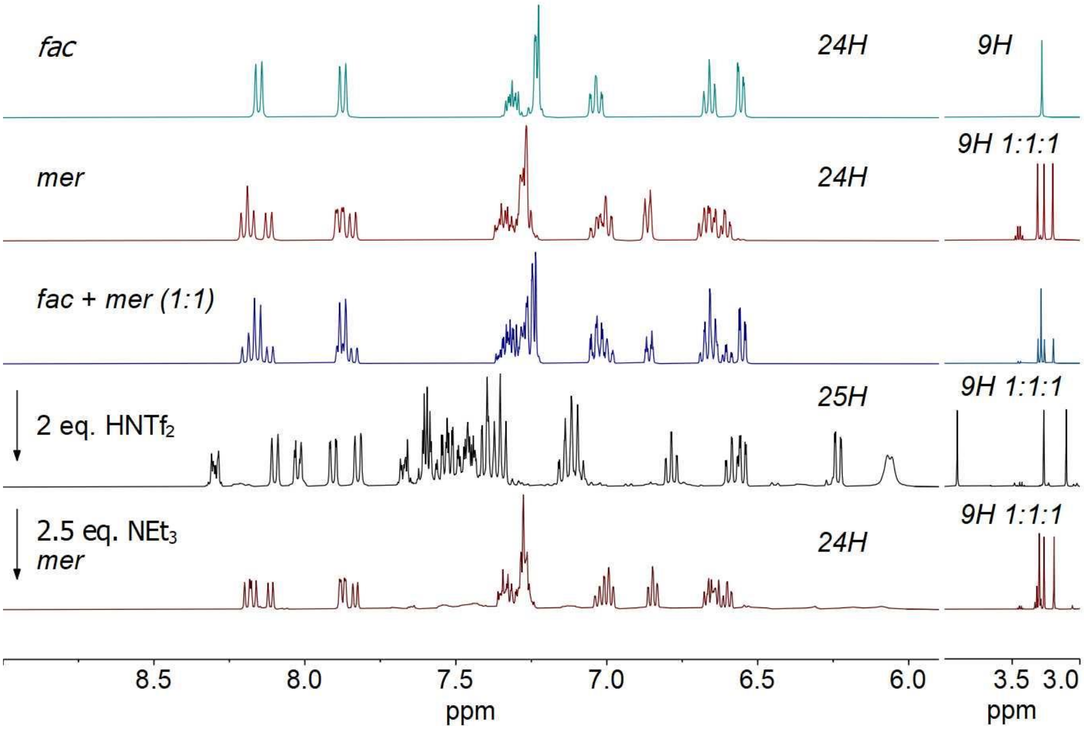

Figure S6. ^{1}H (400 MHz, CD$_2$Cl$_2$) NMR spectra of *fac* and *mer* isomers of Ir(pmb)$_3$ and the conversion of mixture of *fac* and *mer* to *mer* through [Ir(pmb)(Hpmb)](NTf$_2$).

The same experiment was performed for the mixture of *fac*-Ir(pbb)$_3$ and *mer*-Ir(pbb)$_3$. The corresponding NMR spectra are shown in Figure S7.

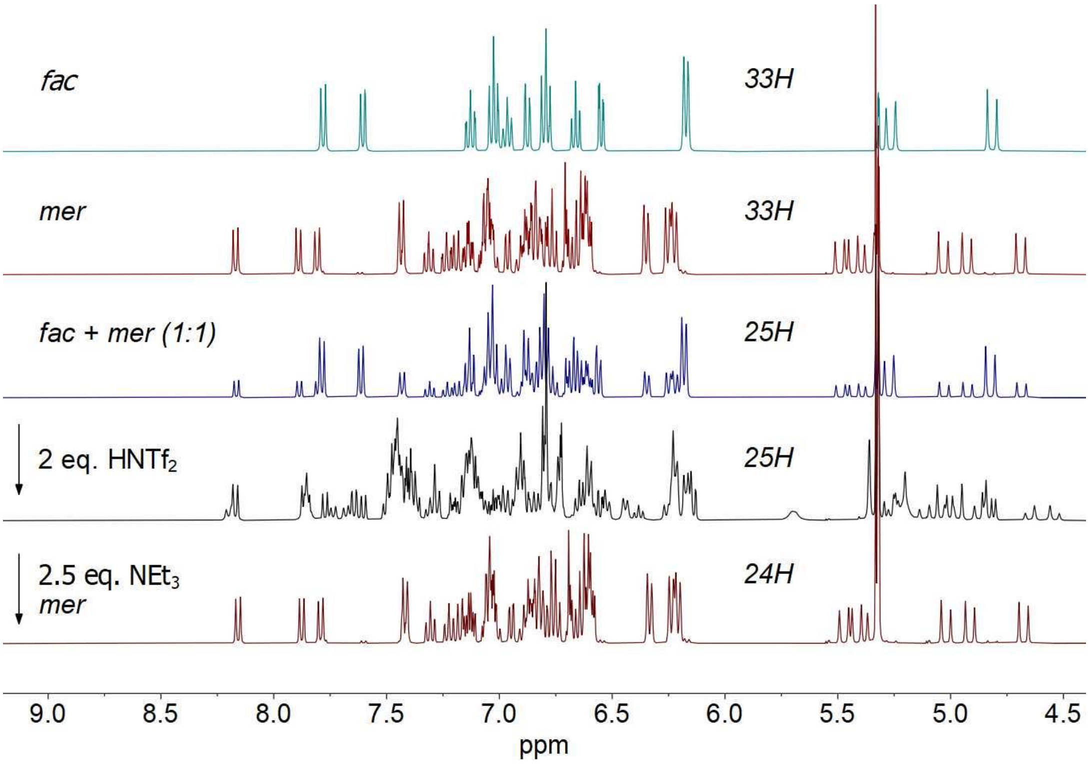

Figure S7. ^{1}H (400 MHz, CD_2Cl_2) NMR spectra of *fac* and *mer* isomers of $Ir(pbb)_3$ and the conversion of mixture of *fac* and *mer* to *mer* through $[Ir(pbb)_2(Hpbb)](NTf_2)$.

Crystallographic data

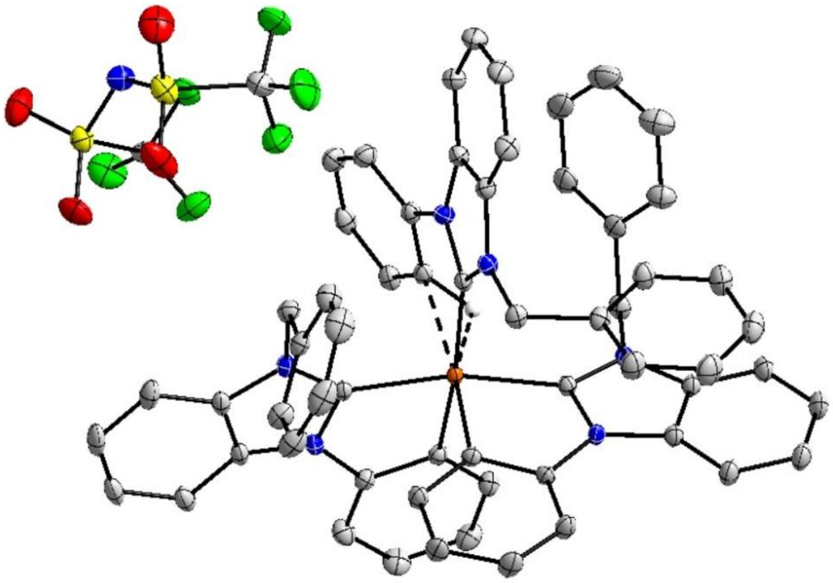

Figure S8. ORTEP view of **[Ir(pmb)$_2$(Hpmb)](NTf$_2$)** at the 50% probability level. Most hydrogen atoms are omitted for clarity.

Structure Quality Indicators

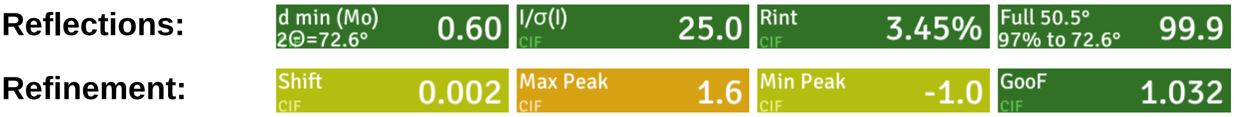

Reflections:	d min (Mo) 2Θ=72.6° 0.60	I/σ(I) CIF 25.0	Rint CIF 3.45%	Full 50.5° 97% to 72.6° 99.9
Refinement:	Shift CIF 0.002	Max Peak CIF 1.6	Min Peak CIF -1.0	GooF CIF 1.032

A clear intense yellow prism-shaped crystal with dimensions of 0.16 × 0.09 × 0.04 mm^3 was mounted. Data were collected using an XtaLAB Synergy R, DW system, HyPix-Arc 150 diffractometer operating at T = 140.00(10) K.

Data were measured using ω scans using Mo$K\alpha$ radiation. The diffraction pattern was indexed and the total number of runs and images was based on the strategy calculation from the program CrysAlis^{Pro} 1.171.42.70a (CrysAlis^{Pro} Software System, Rigaku Oxford Diffraction, 2022).[5] The maximum resolution that was achieved was Θ = 36.319° (0.60 Å).

The unit cell was refined using CrysAlis^{Pro} 1.171.42.70a on 36919 reflections, 46 % of the observed reflections.

Data reduction, scaling and absorption corrections were performed using CrysAlis^{Pro} 1.171.42.70a. The final completeness is 99.90 % out to 36.319° in Θ. A Gaussian absorption correction was performed using CrysAlis^{Pro} 1.171.42.70a. Numerical absorption correction based on gaussian integration over a multifaceted crystal model Empirical absorption correction using spherical harmonics, implemented in SCALE3 ABSPACK scaling algorithm. The absorption coefficient μ of this material is 2.748 mm^{-1} at this wavelength (λ = 0.71073 Å) and the minimum and maximum transmissions are 0.770 and 0.991.

The structure was solved in the space group $P\bar{1}$ (# 2) by the ShelXT 2018/2[6] structure solution program using dual methods and refined by full-matrix least-squares minimization on F^2 using version 2018/3 of ShelXL 2018/3.[7] All non-hydrogen atoms were refined anisotropically. The hydrogen atom positions were calculated geometrically and refined using the riding model, but the hydride was found in a difference map and refined freely.

There is a single molecule in the asymmetric unit, which is represented by the reported sum formula. In other words: *Z* is 2 and *Z'* is 1.

Data Plots: Diffraction Data

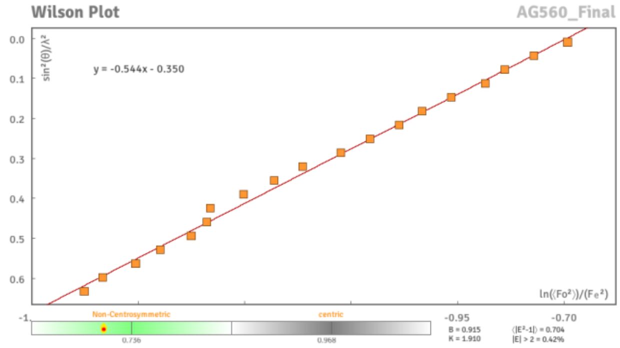

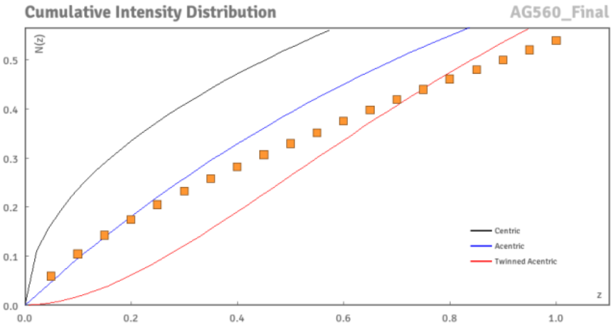

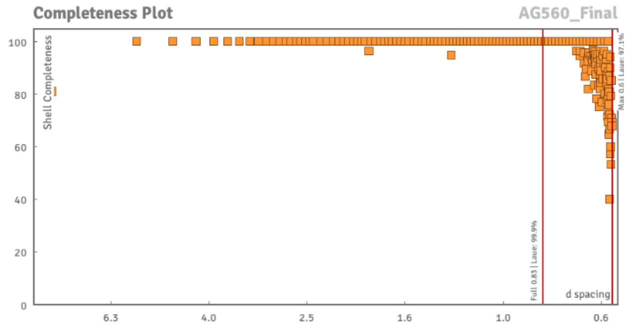

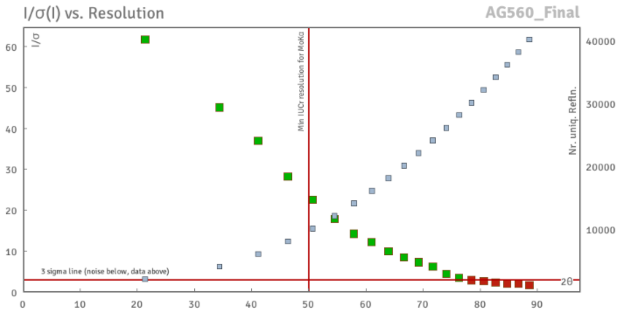

Data Plots: Refinement and Data

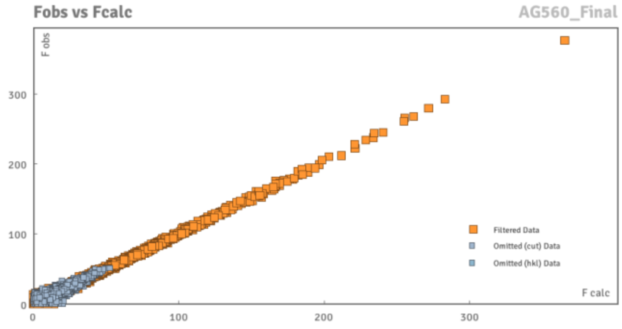

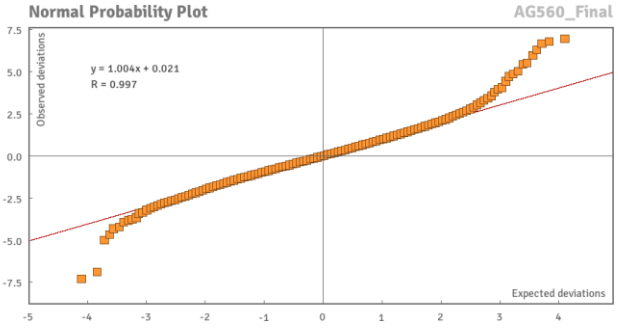

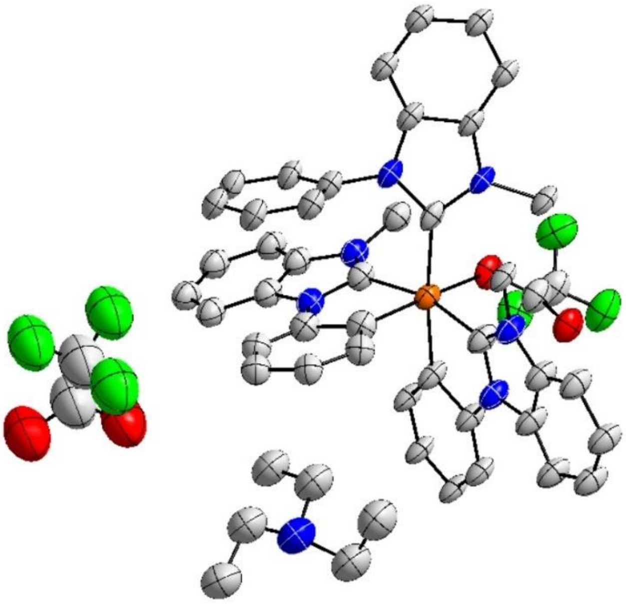

Figure S9. ORTEP view of Ir(pmb)$_2$(Hpmb)(CO$_2$CF$_3$) with (NHEt$_3$)(CO$_2$CF$_3$) trapped in the crystal cell at the 50% probability level. Hydrogen atoms are omitted for clarity.

Structure Quality Indicators

Reflections:	d min (Cu\a) 2Θ=89.2° 1.10	I/σ(I) CIF 11.4	Rint CIF n/a	Full 89.2° 97.0
Refinement:	Shift CIF 0.000	Max Peak CIF 2.0	Min Peak CIF -1.5	GooF CIF 1.114

A colourless plate-shaped crystal with dimensions of 0.19 × 0.05 × 0.04 mm^3 was mounted. Data were collected using an XtaLAB Synergy R, DW system, HyPix-Arc 150 diffractometer operating at T = 140.00(10) K.

Data were measured using ω scans with Cu$K\alpha$ radiation. The diffraction pattern was indexed, and the total number of runs and images was based on the strategy calculation from the program CrysAlisPro 1.171.42.75a (Rigaku OD, 2022). The maximum resolution achieved was Θ = 44.586° (1.10 Å).

The unit cell was refined using CrysAlis^{Pro} 1.171.42.75a (Rigaku OD, 2022) on 3930 reflections, 62% of the observed reflections.

Data reduction, scaling and absorption corrections were performed using CrysAlis^{Pro} 1.171.42.75a (Rigaku OD, 2022). The final completeness is 97.00 % out to 44.586° in Θ. A Gaussian absorption correction was performed using CrysAlis^{Pro} 1.171.42.75a (Rigaku Oxford Diffraction, 2022) Numerical absorption correction was based on Gaussian integration over a multifaceted crystal model. Empirical absorption correction using spherical harmonics as implemented in SCALE3 ABSPACK scaling algorithm. The absorption coefficient μ of this material is 5.137 mm^{-1} at this wavelength (λ = 1.54184Å) and the minimum and maximum transmissions are 0.513 and 1.000.

The structure was solved in the space group $P2_1/c$ (# 14) by the ShelXT 2018/2 (Sheldrick, 2015) structure solution program using dual methods and refined by full-matrix least-squares minimisation on $\boldsymbol{F^2}$ using version 2018/3 of **ShelXL** 2018/3

(Sheldrick, 2015). All non-hydrogen atoms were refined anisotropically. Hydrogen atom positions were calculated geometrically and refined using the riding model.

_refine_special_details: Refined as a 2-component twin.

_twin_special_details: Component 2 rotated by -179.9022° around [0.00 1.00 0.00] (reciprocal) or [0.07 1.00 0.01] (direct)

_platon_squeeze_special_details: A solvent mask was calculated, and 414 electrons were found in a volume of 1171 Å^3 in two voids per unit cell. This is consistent with the presence of 2.5 solvent molecules of pentane per asymmetric unit which account for 336 electrons per unit cell.

There is a single molecule in the asymmetric unit, represented by the reported sum formula. In other words: Z is 4 and Z' is 1.

The crystal was weakly-diffracting, perhaps because of [100] channels in the structure. The resolution reported is the best which could be achieved, even though the crystal data were collected up to 0.83 Angstrom resolution, the crystal (the largest available) still diffracted quite weakly at high angle, possibly because of the big number of disordered solvent molecules.

Data Plots: Diffraction Data

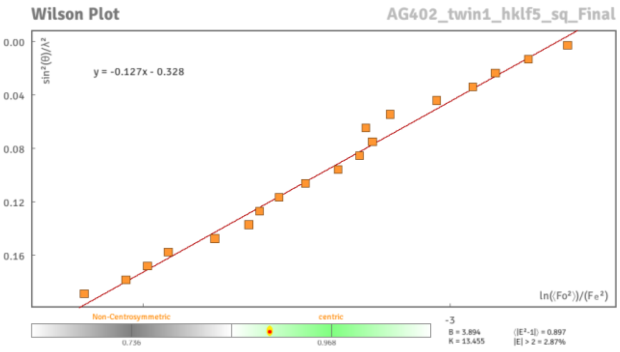

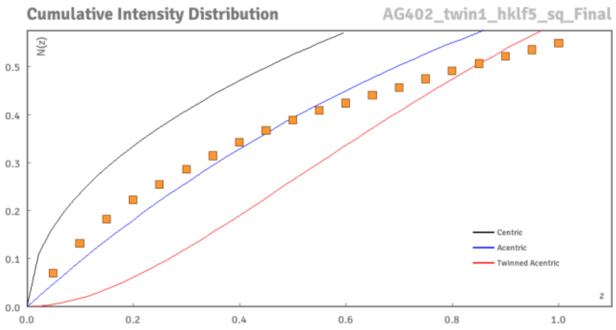

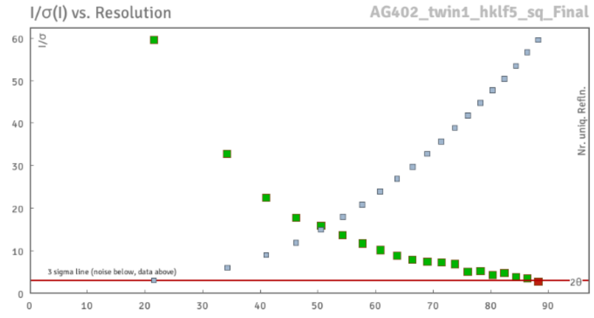

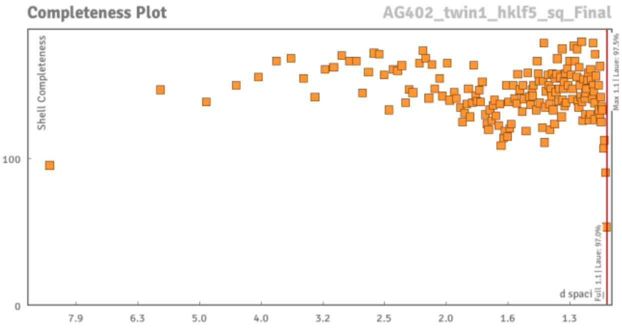

Data Plots: Refinement and Data

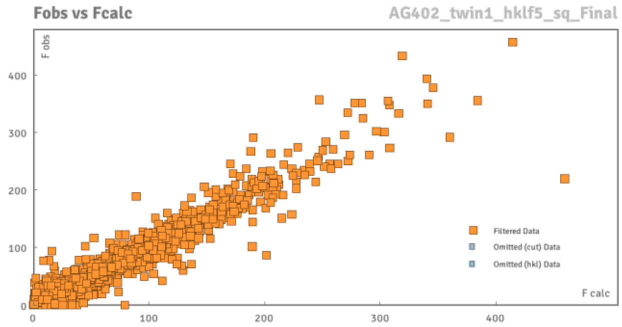

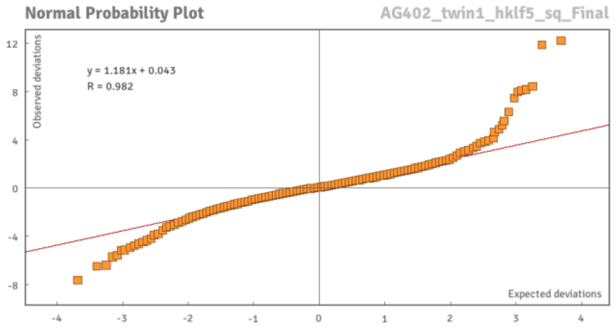

Table S2. Crystallographic data of the compounds.

Compound	[Ir(pmb)$_2$(Hpmb)](NTf$_2$)	Ir(pmb)$_2$(Hpmb)(CO$_2$CF$_3$)
Formula	$C_{62}H_{46}F_6IrN_7O_4S_2$	$C_{52}H_{50}F_6IrN_7O_4$
Formula Weight	1.702	1.345
$D_{calc.}$, g cm^{-3}	2.748	5.137
μ, mm^{-1}	1323.38	1143.19
Colour	clear intense yellow	colourless
Shape	prism-shaped	plate-shaped
Size, mm^3	0.16 × 0.09 × 0.04	0.19×0.05×0.04
T, K	140.00(10)	140.00(10)
Crystal System	triclinic	monoclinic
Space Group	$P\bar{1}$	$P2_1/c$
a, Å	11.63227(10)	9.2601(8)
b, Å	13.80526(10)	37.467(3)
c, Å	16.19706(13)	16.6652(12)
α, °	85.2923(6)	90
β, °	87.1337(7)	102.416(9)
γ, °	85.6362(7)	90
V, Å^3	2582.23(4)	5646.7(8)
Z	2	4
Z'	1	1
λ, Å	0.71073	1.54184
Radiation type	Mo$K\alpha$	Cu$K\alpha$
Θ_{min}, °	2.023	2.960
Θ_{max}, °	36.319	44.586
Measured Refl.	80489	6384
Independent Refl.	24306	6384
Refl. $I \geq 2\sigma(I)$	21440	4301
R_{int}	0.0345	n/a
Parameters	743	638
Restraints	0	1034
Largest Peak, e Å^{-3}	1.568	2.025
Deepest Hole, e Å^{-3}	-0.982	-1.495
GooF	1.032	1.114
wR_2 (all data)	0.0608	0.2932
wR_2	0.0590	0.2574
R_1 (all data)	0.0373	0.1429
R_1	0.0288	0.1021
CCDC number	*2210250*	*2225294*

NMR spectra

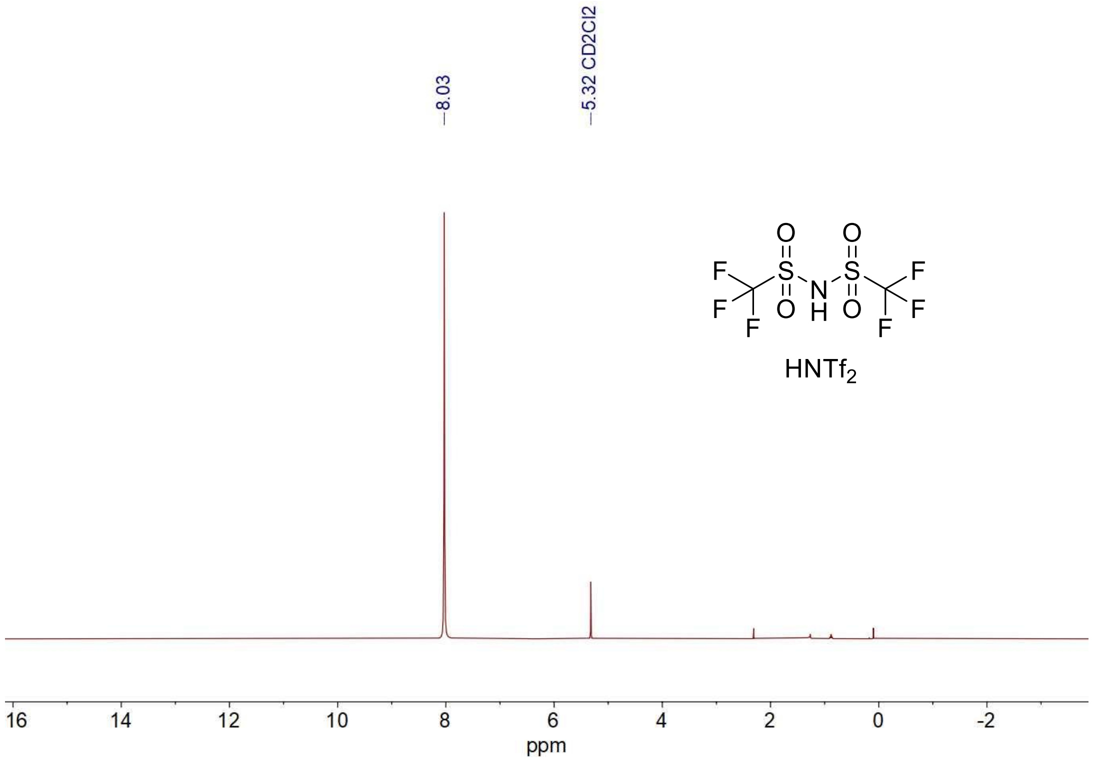

^1H NMR (400 MHz, CD_2Cl_2, 298 K) spectrum of $HNTf_2$

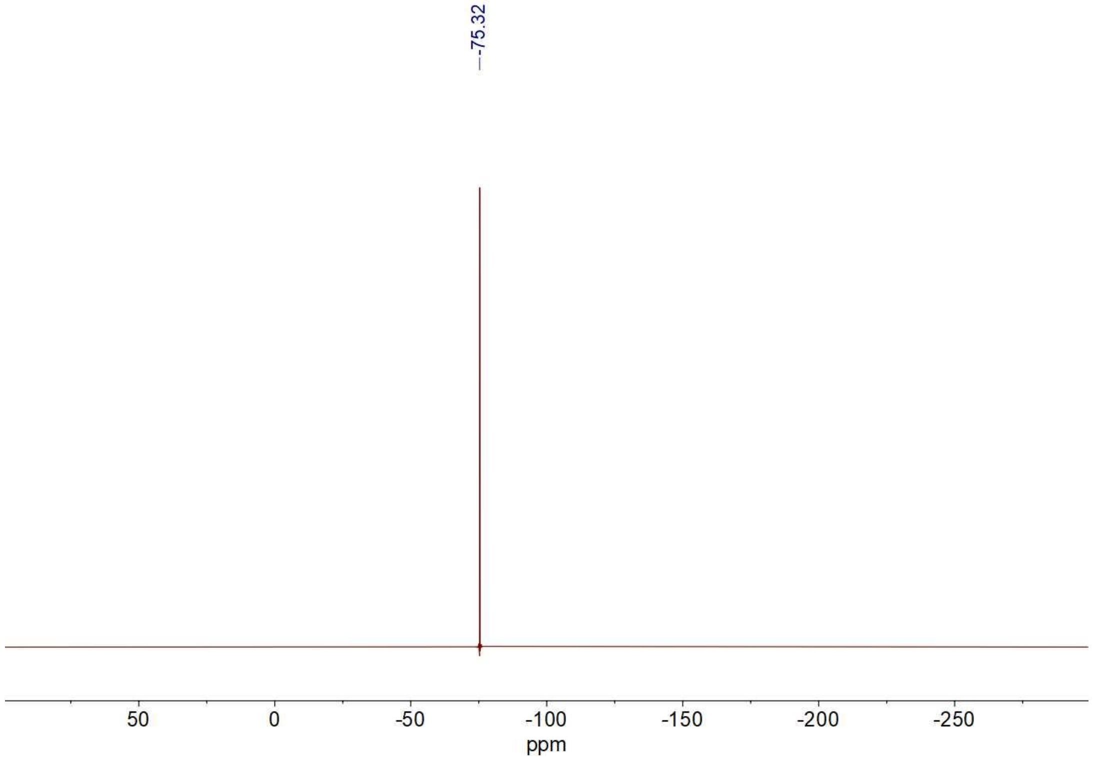

^{19}F NMR (376 MHz, CD_2Cl_2, 298 K) spectrum of $HNTf_2$

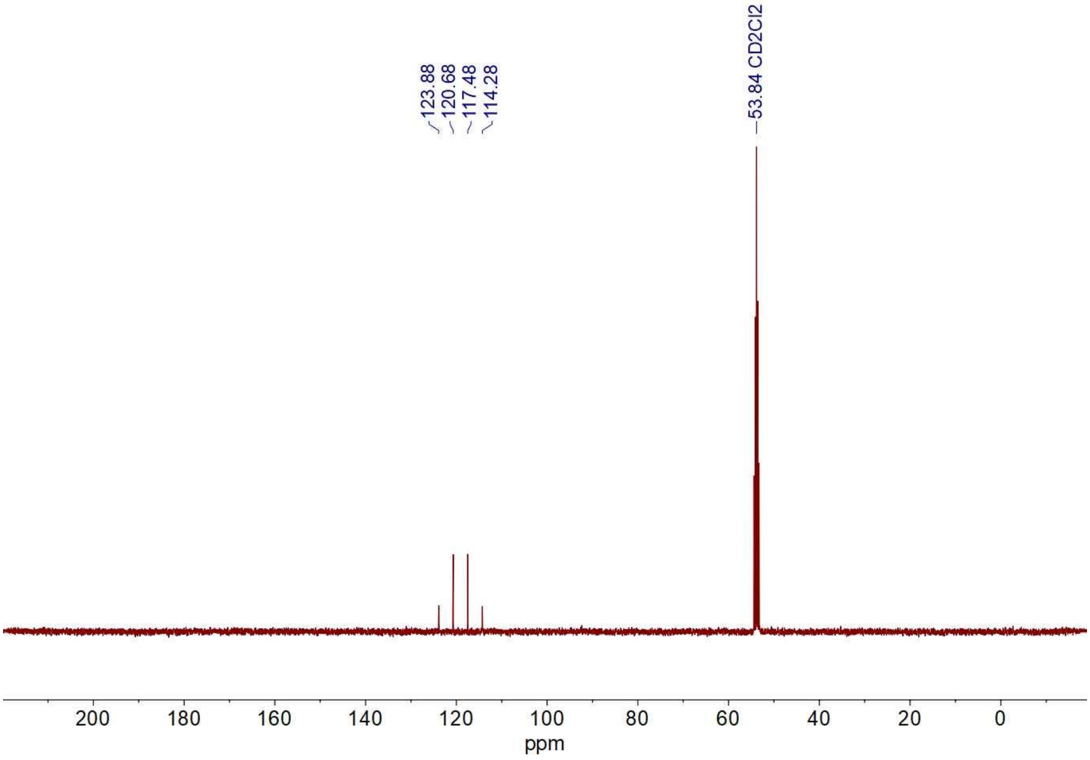

^{13}C NMR (101 MHz, CD_2Cl_2, 298 K) spectrum of $HNTf_2$

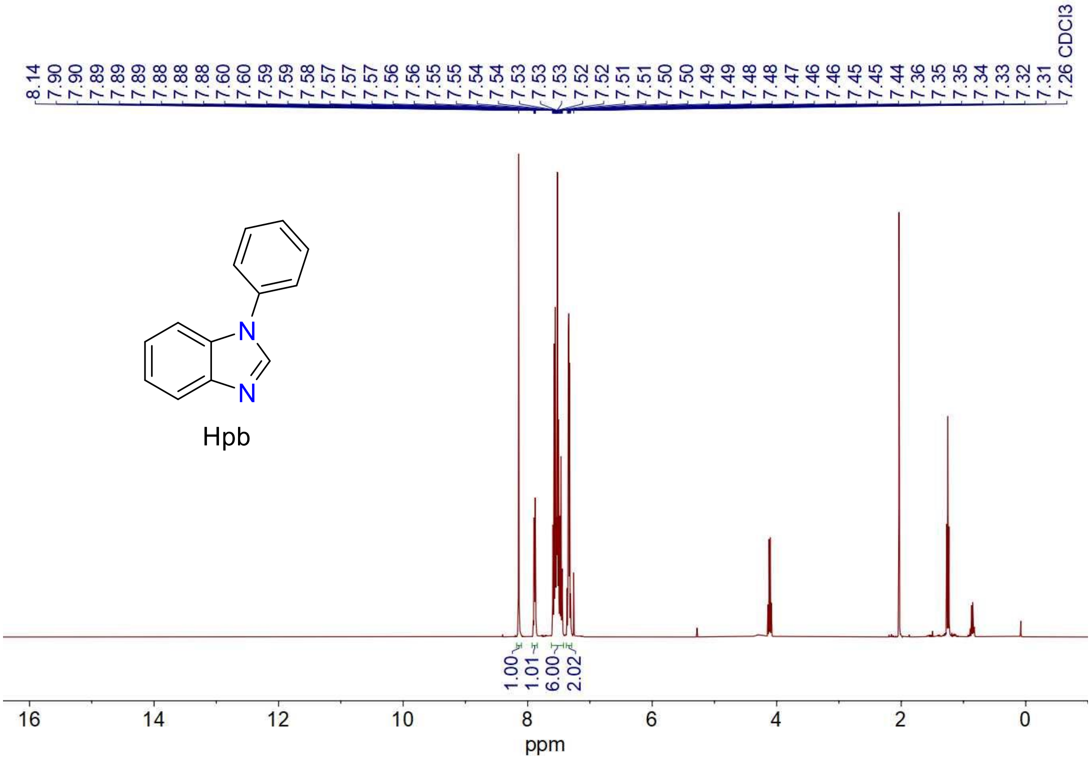

^{1}H NMR (400 MHz, CD_2Cl_2, 298 K) spectrum of Hpb

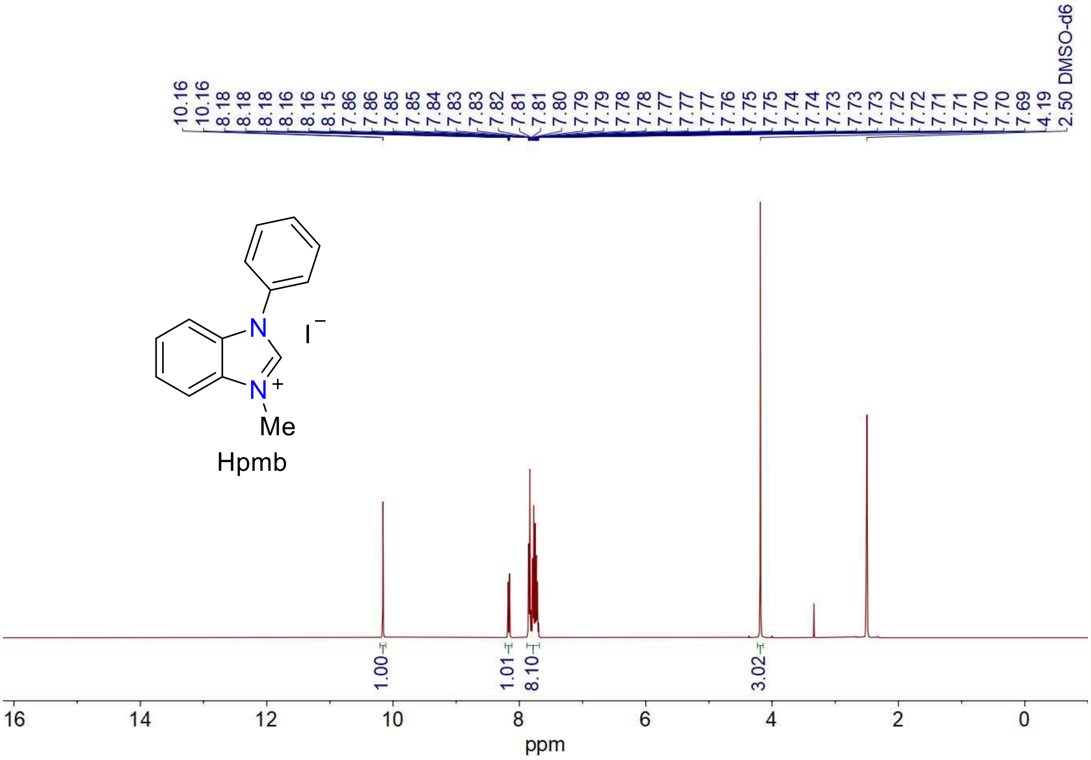

^{1}H NMR (400 MHz, DMSO-d$_6$, 298 K) spectrum of Hpmb

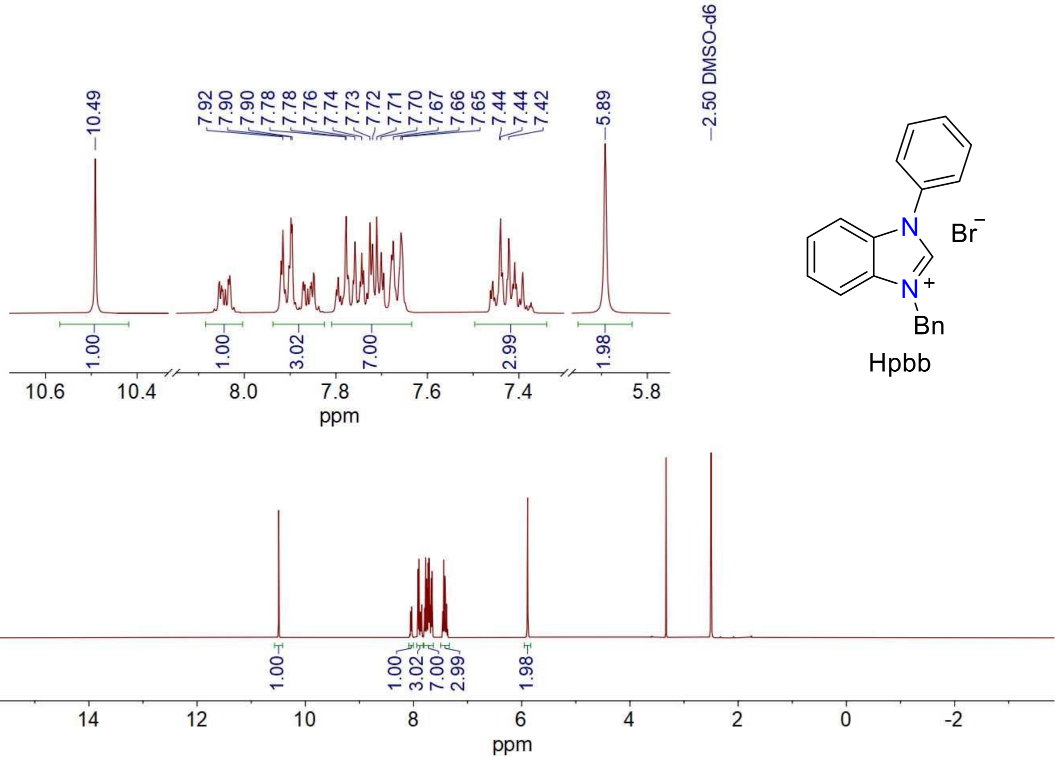

^{1}H NMR (400 MHz, DMSO-d$_6$, 298 K) spectrum of Hpbb

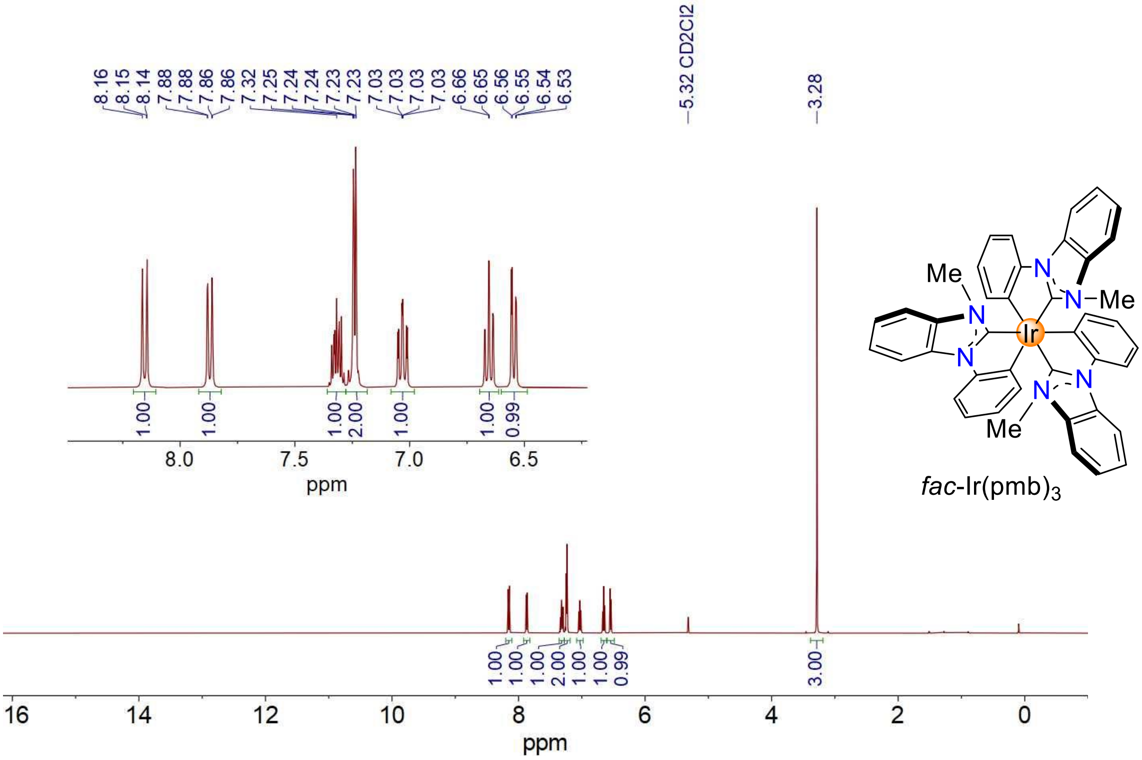

^{1}H NMR (400 MHz, CD_2Cl_2, 298 K) spectrum of *fac*-Ir(pmb)$_3$

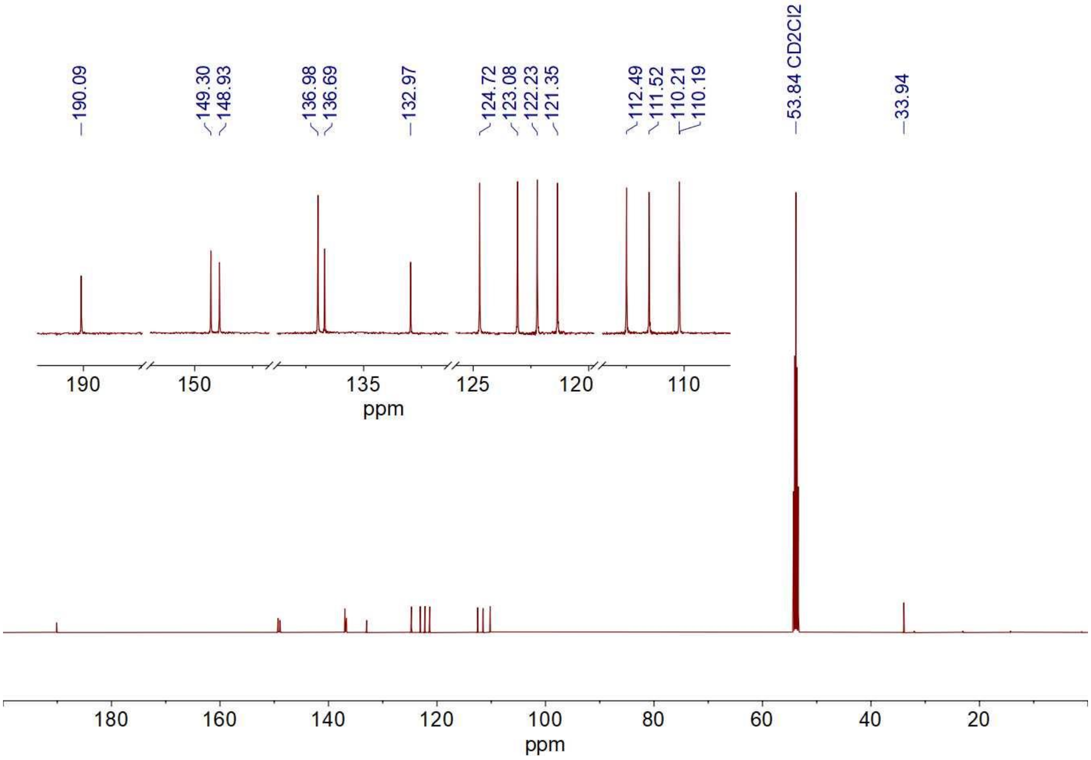

^{13}C NMR (126 MHz, CD_2Cl_2, 298 K) spectrum of *fac*-Ir(pmb)$_3$

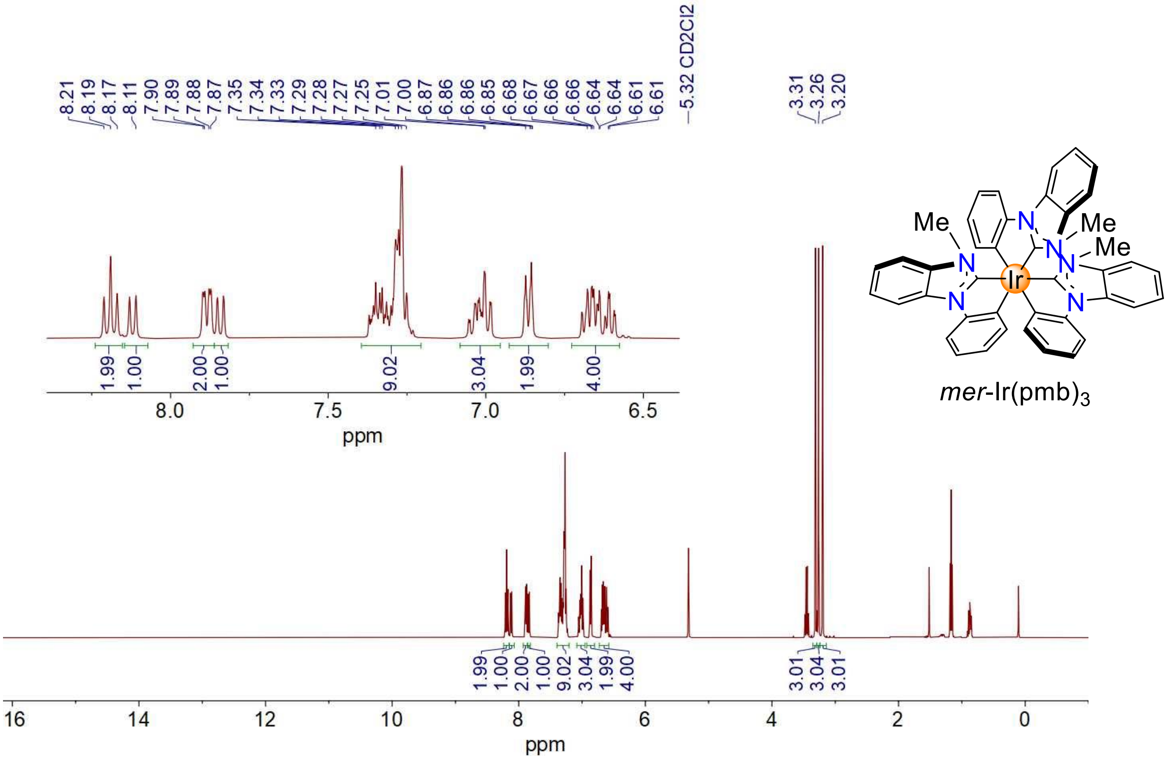

^{1}H NMR (400 MHz, CD_2Cl_2, 298 K) spectrum of *mer*-Ir(pmb)$_3$

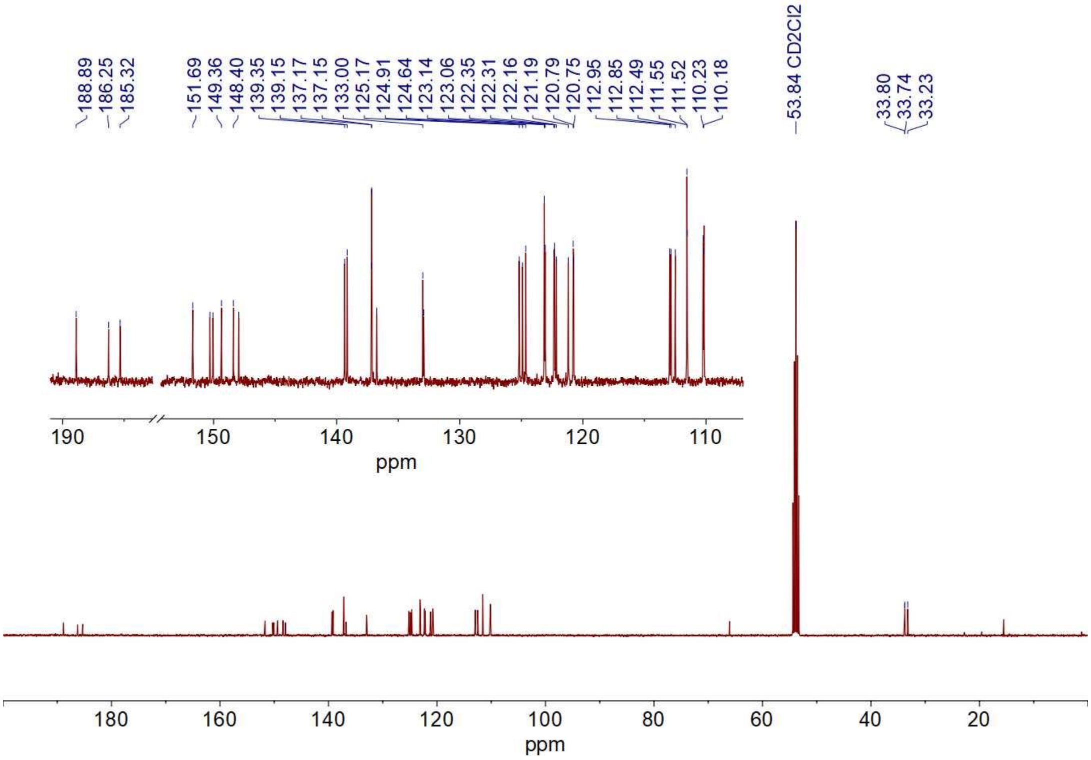

^{13}C NMR (101 MHz, CD_2Cl_2, 298 K) spectrum of *mer*-Ir(pmb)$_3$

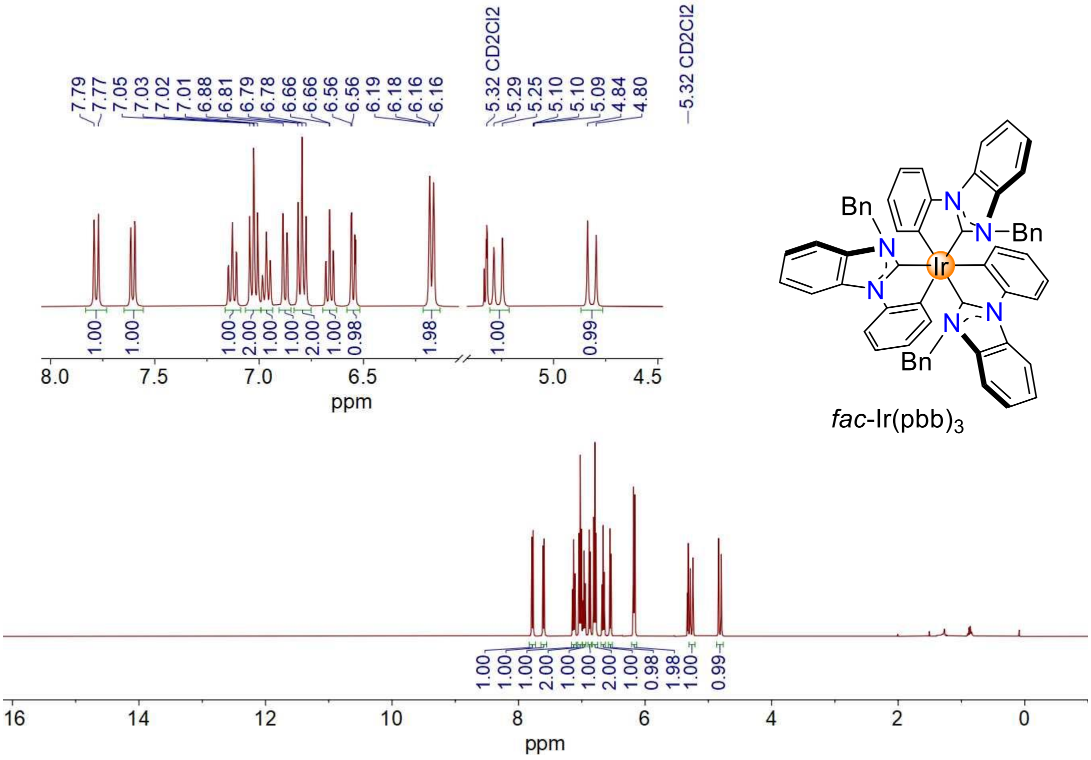

^{1}H NMR (400 MHz, CD$_2$Cl$_2$, 298 K) spectrum of *fac*-Ir(pbb)$_3$

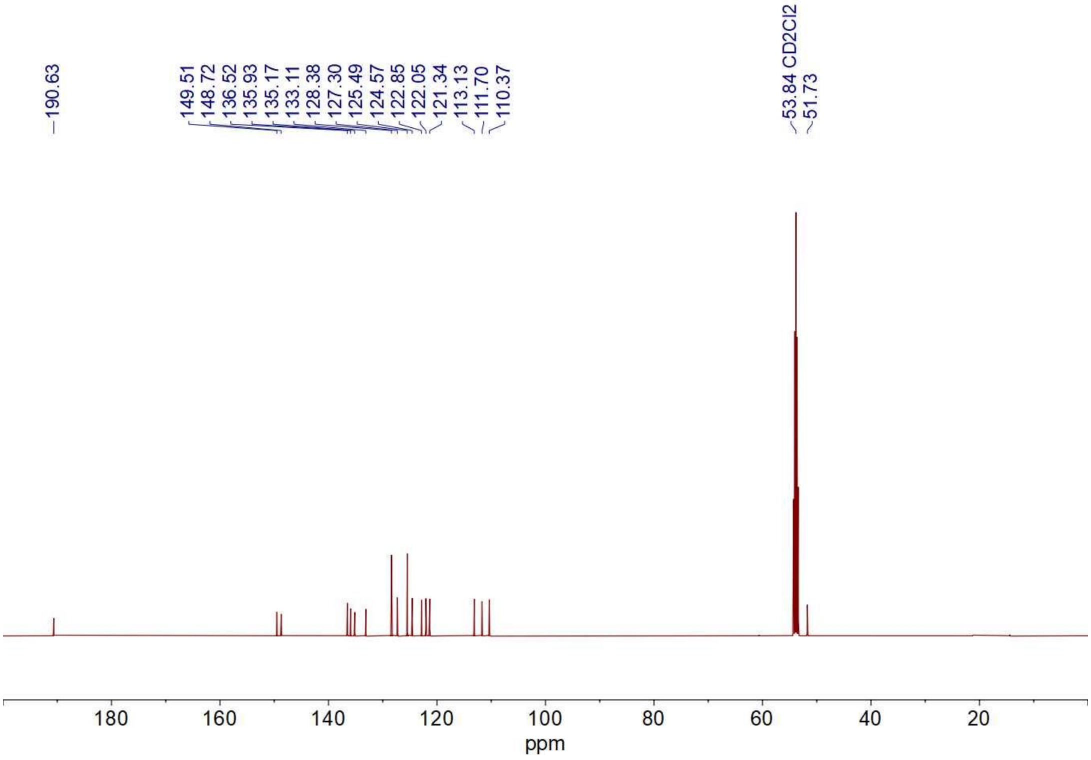

^{13}C NMR (126 MHz, CD$_2$Cl$_2$, 298 K) spectrum of *fac*-Ir(pbb)$_3$

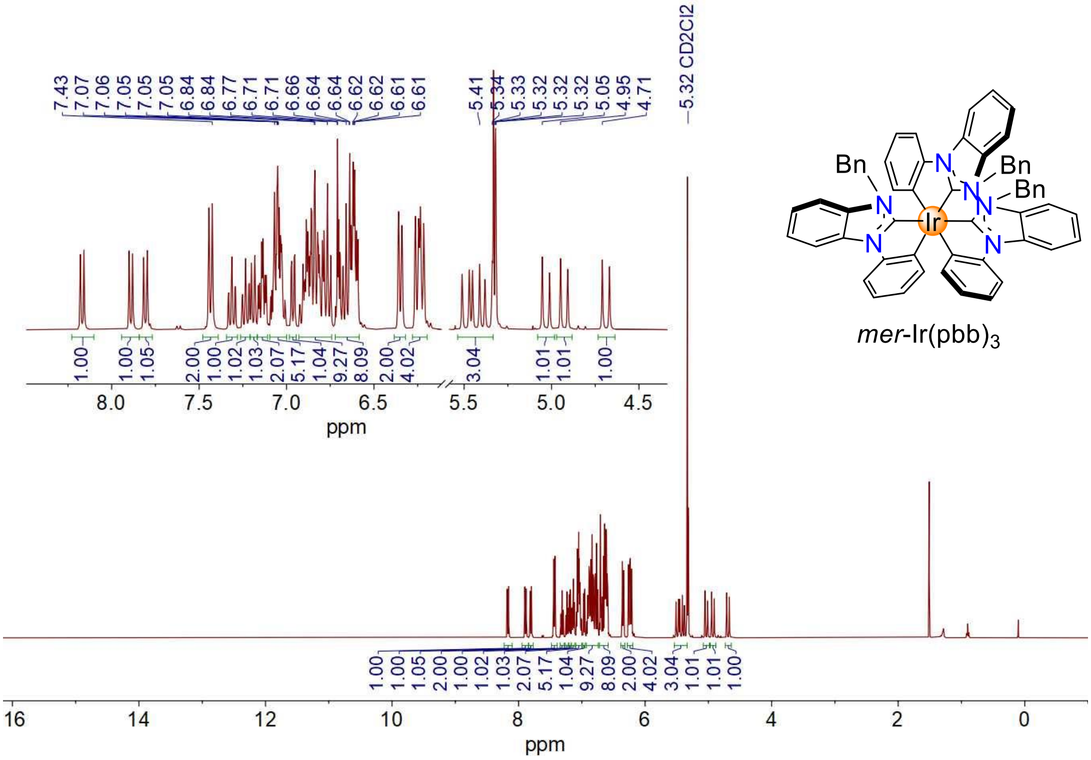

^{1}H NMR (400 MHz, CD_2Cl_2, 298 K) spectrum of *mer*-Ir(pbb)$_3$

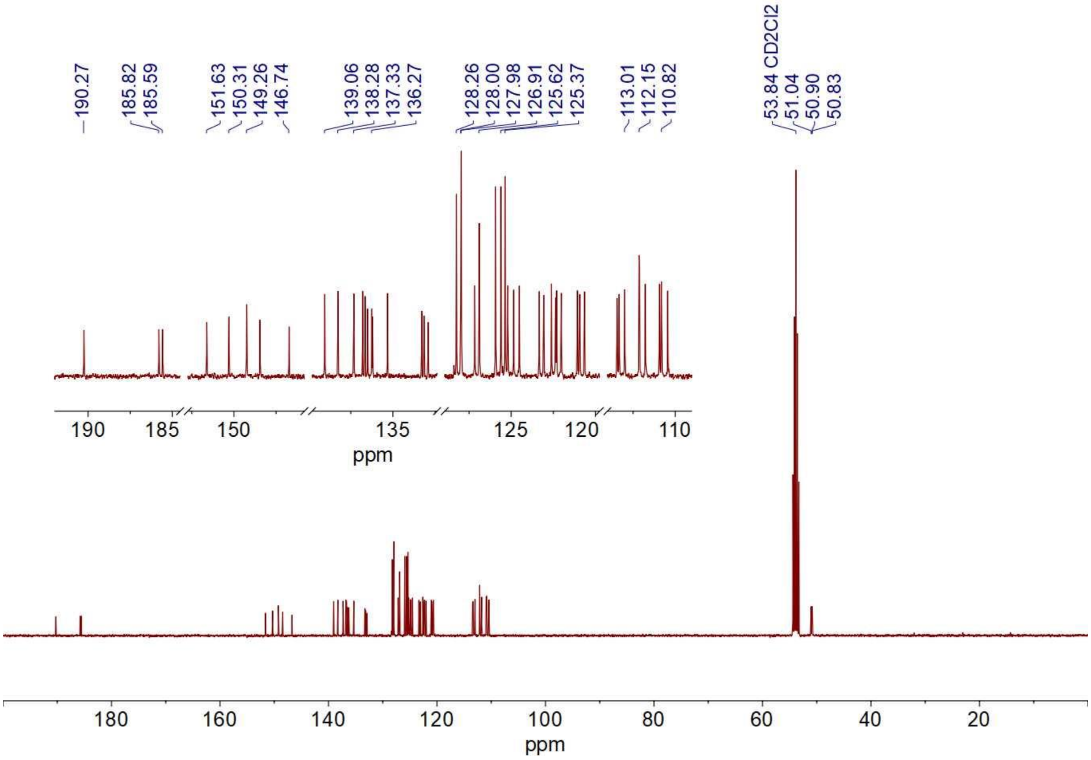

^{13}C NMR (101 MHz, CD_2Cl_2, 298 K) spectrum of *mer*-Ir(pbb)$_3$

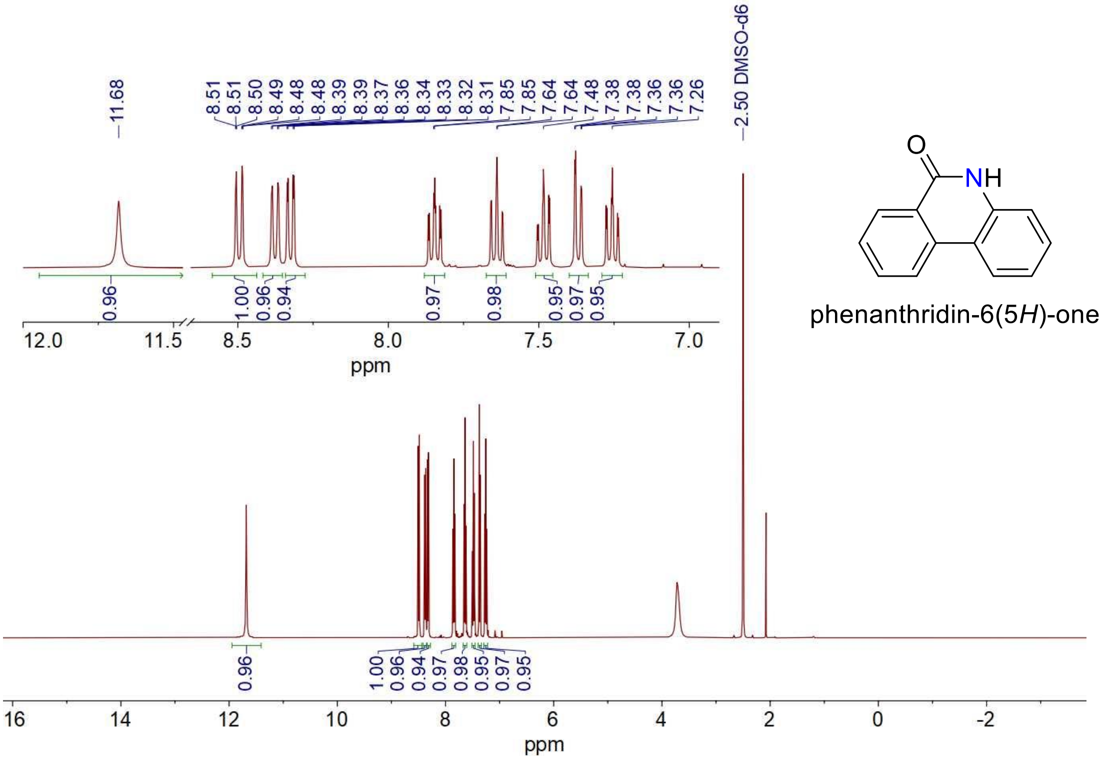

^{1}H NMR (400 MHz, DMSO-d$_6$, 298 K) spectrum of phenanthridine-6(5*H*)-one

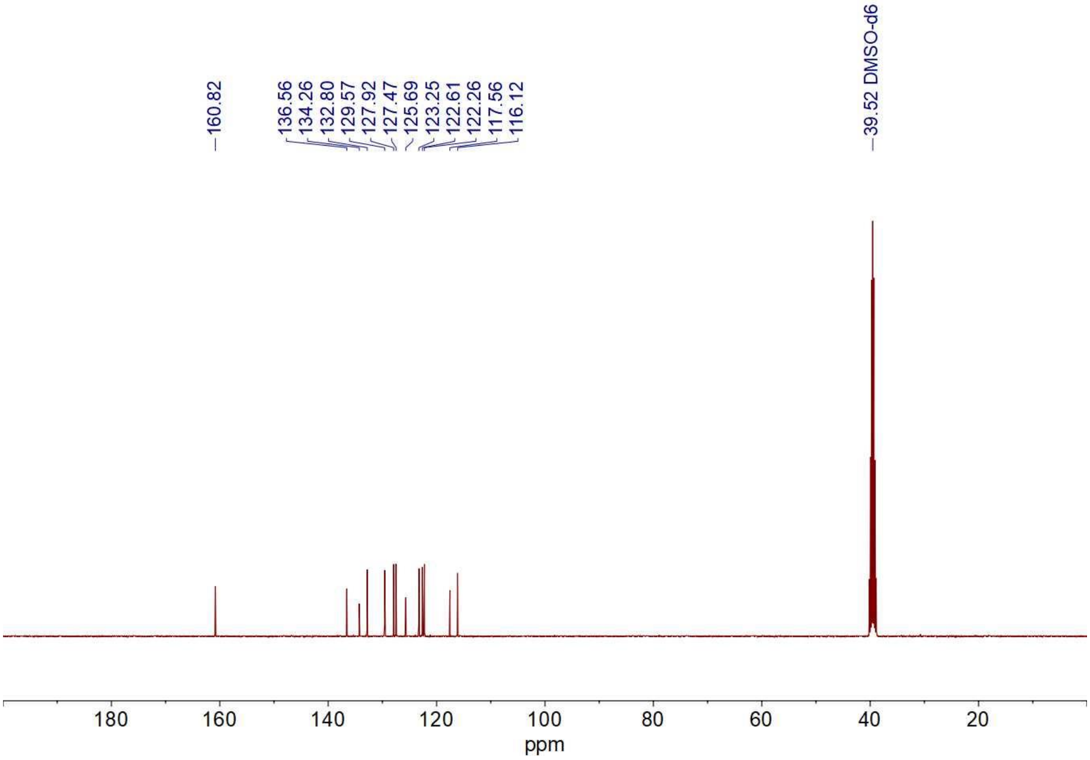

^{13}C NMR (101 MHz, DMSO-d$_6$, 298 K) spectrum of phenanthridine-6(5*H*)-one

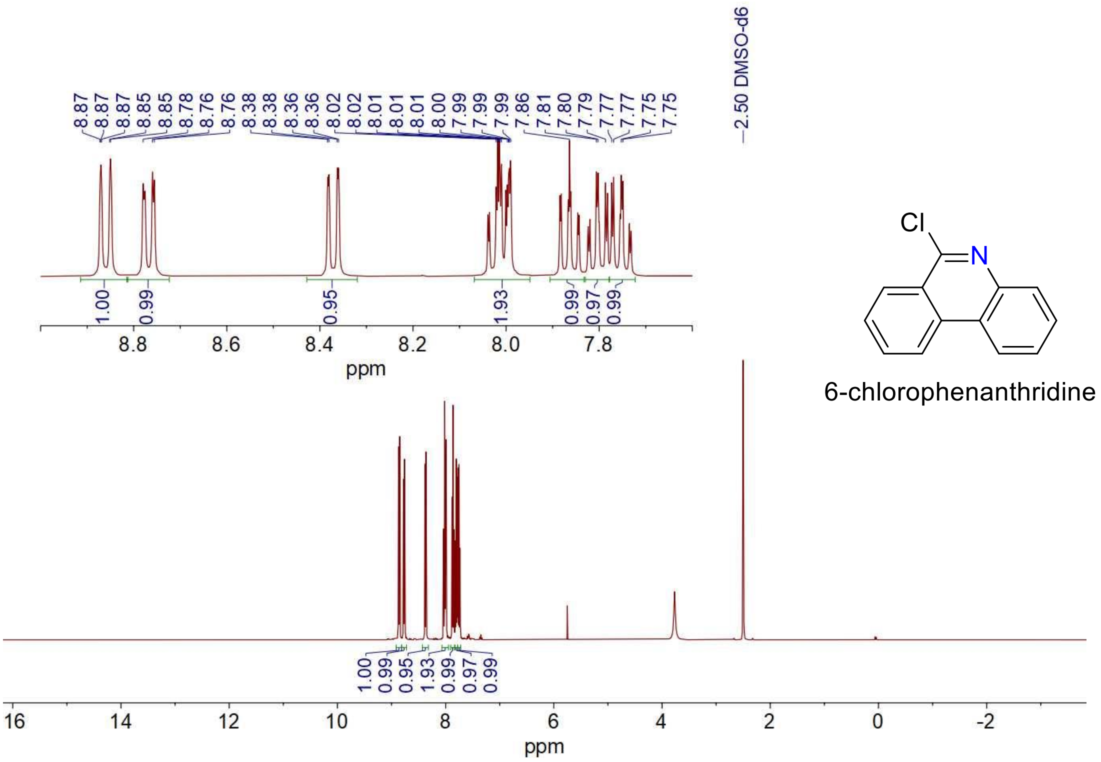

^{1}H NMR (400 MHz, DMSO-d$_6$, 298 K) spectrum of 6-chlorophenanthridine

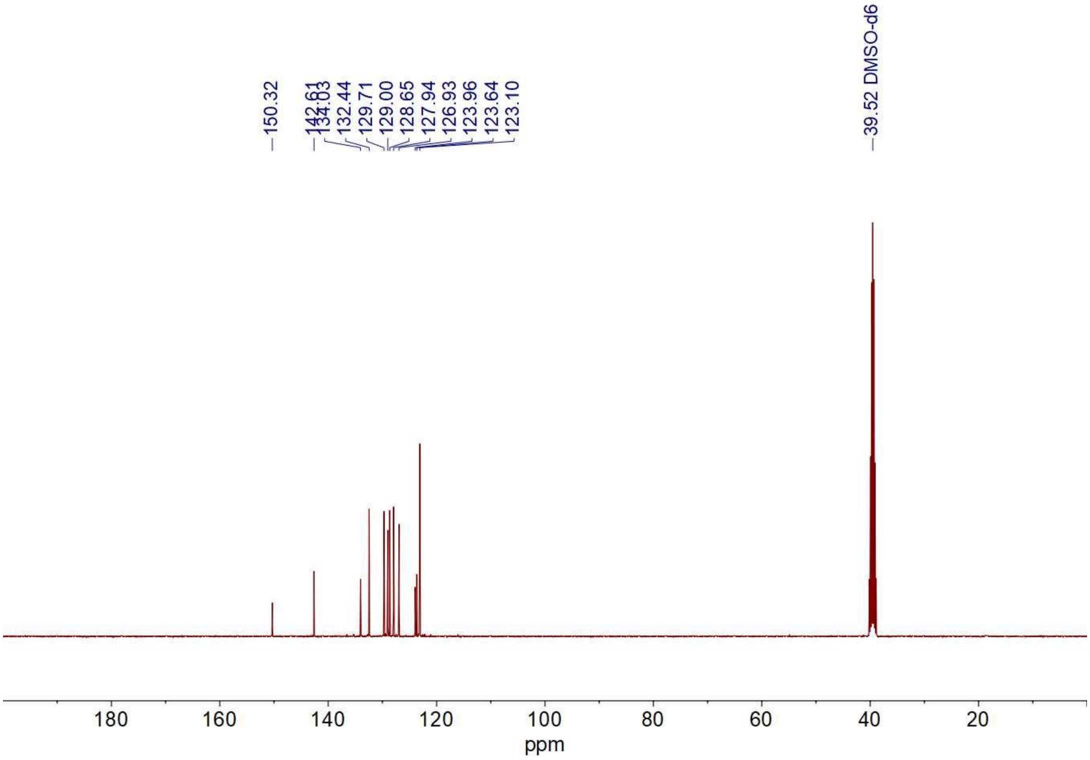

^{13}C NMR (101 MHz, DMSO-d$_6$, 298 K) spectrum of 6-chlorophenanthridine

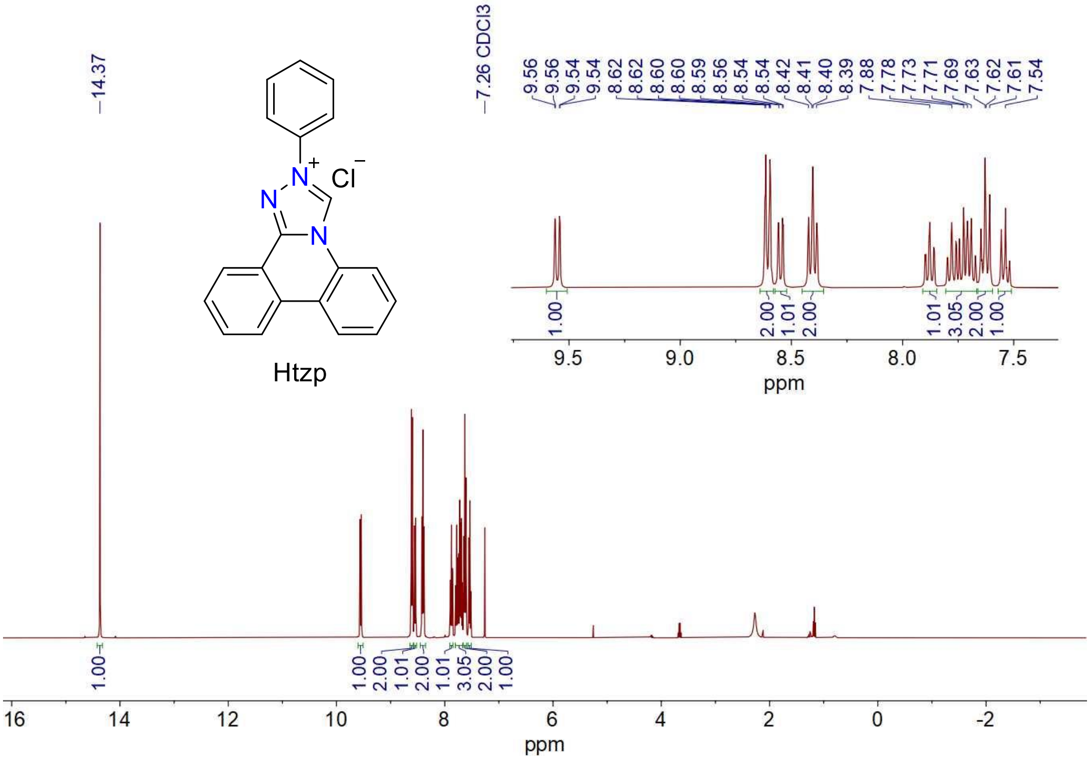

^{1}H NMR (400 MHz, CDCl$_3$, 298 K) spectrum of Htzp

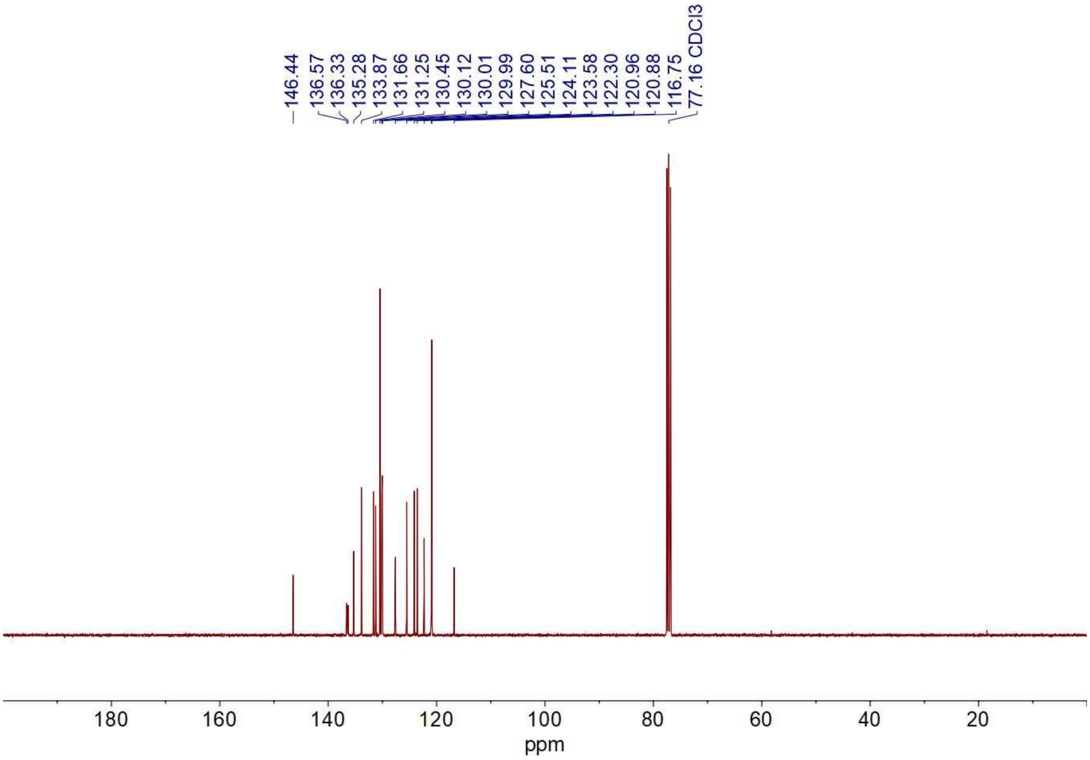

^{13}C NMR (101 MHz, CDCl$_3$, 298 K) spectrum of Htzp

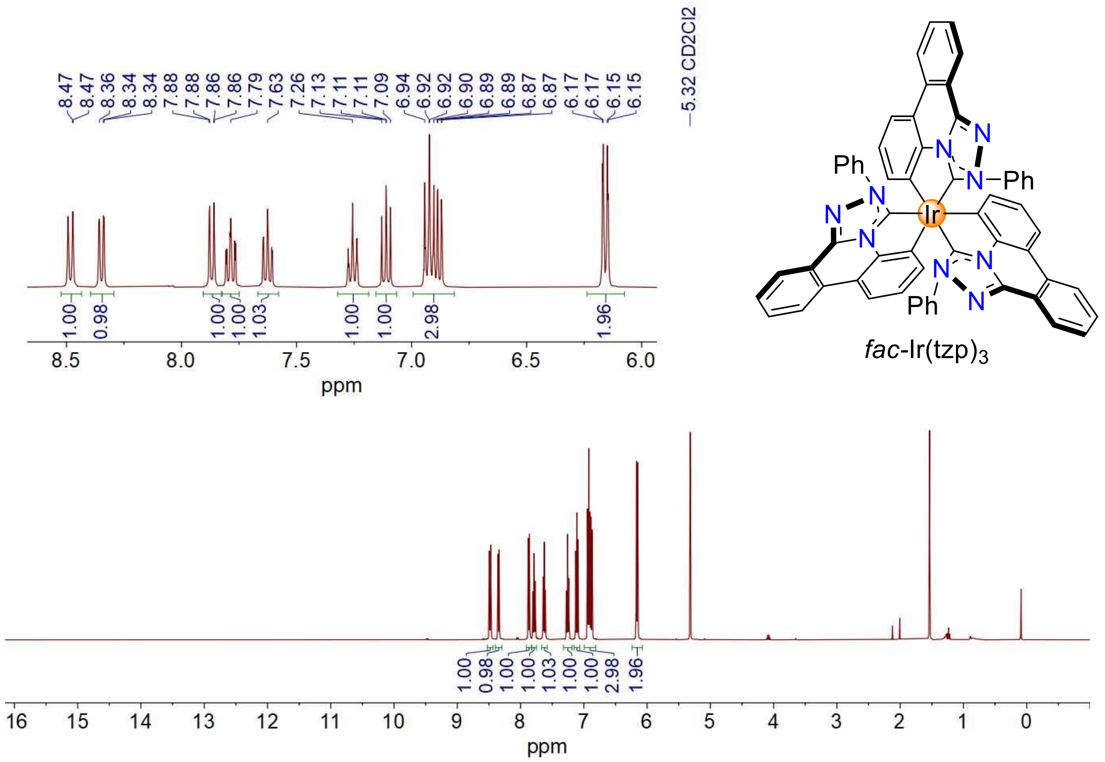

^{1}H NMR (400 MHz, CD_2Cl_2, 298 K) spectrum of *fac*-Ir(tzp)$_3$

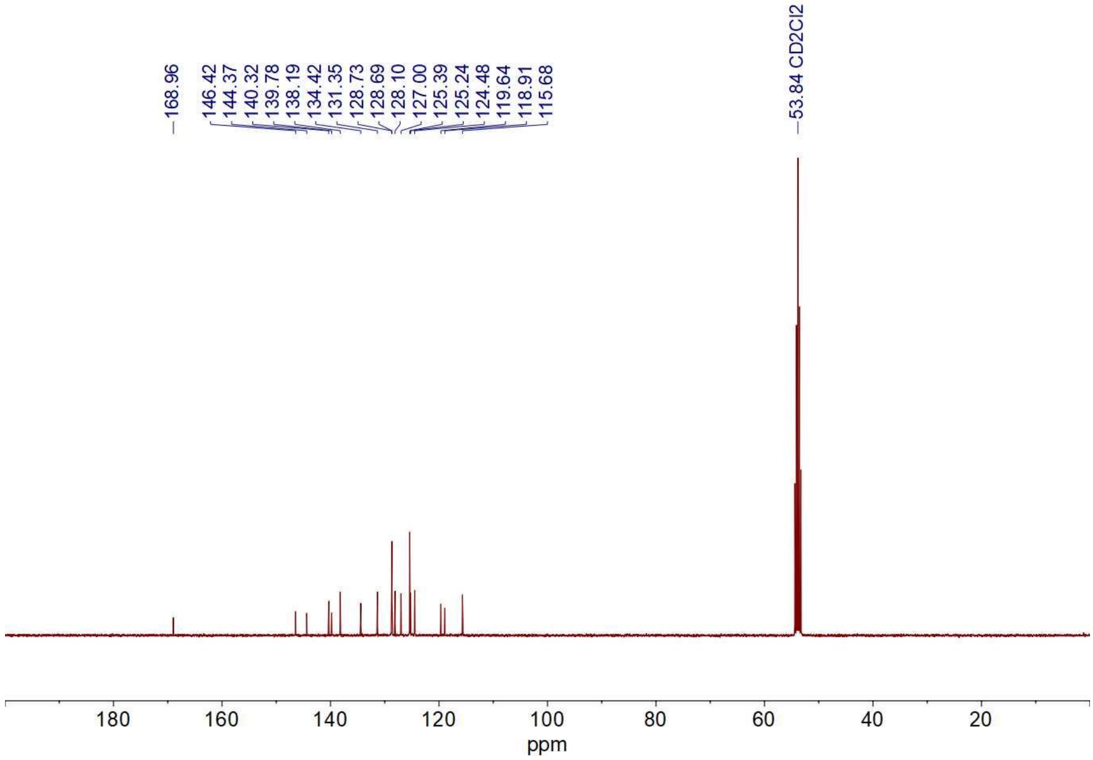

^{13}C NMR (101 MHz, CD_2Cl_2, 298 K) spectrum of *fac*-Ir(tzp)$_3$

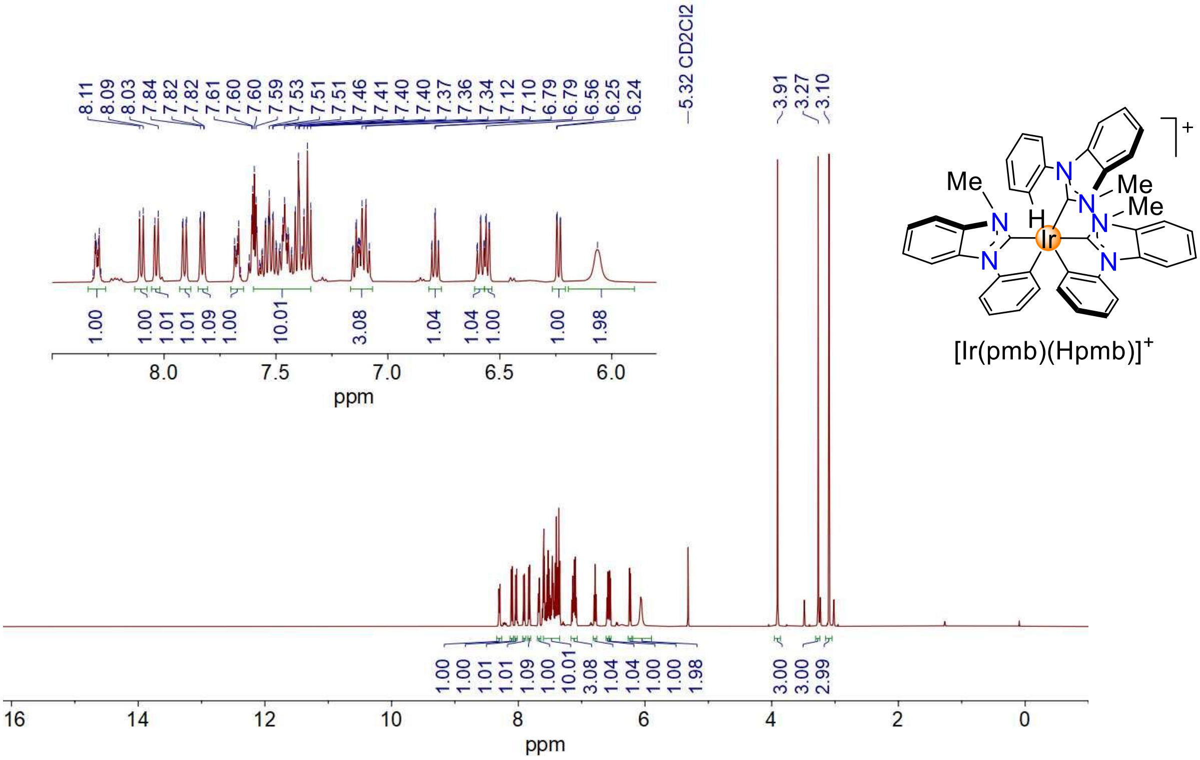

^{1}H NMR (500 MHz, CD_2Cl_2, 298 K) spectrum of [Ir(pmb)$_2$(Hpmb)](NTf_2).

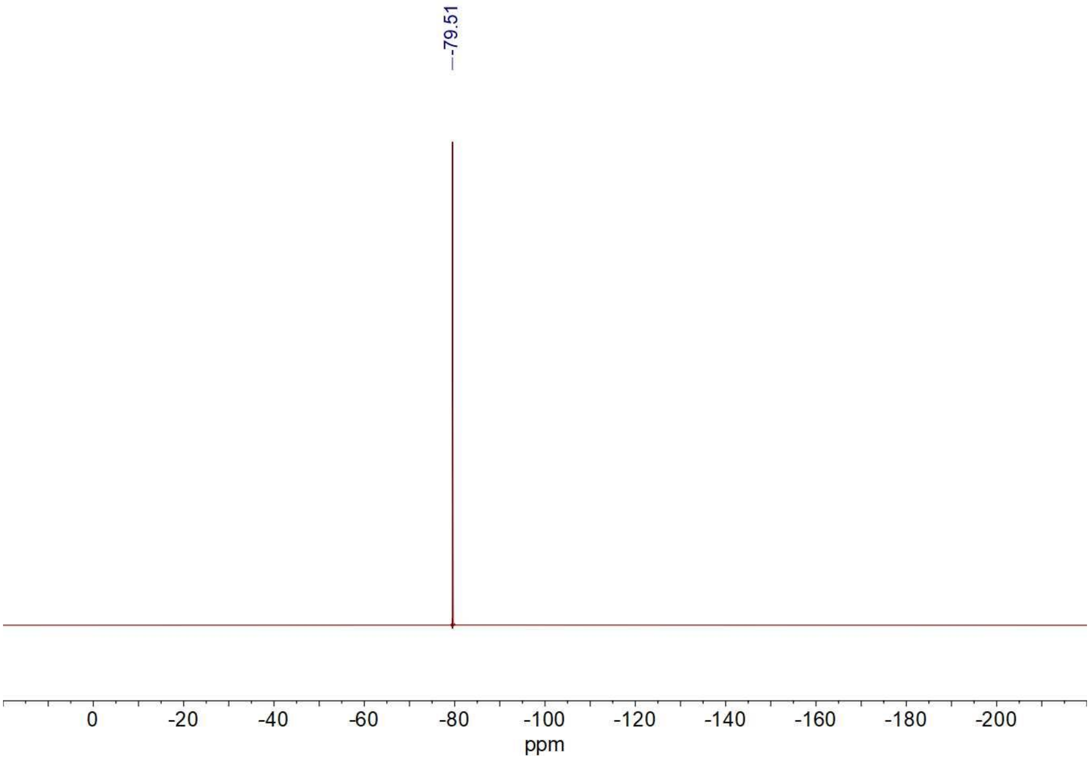

^{19}F NMR (376 MHz, CD_2Cl_2, 298 K) spectrum of [Ir(pmb)$_2$(Hpmb)](NTf_2). The NTf_2 anion is omitted for clarity.

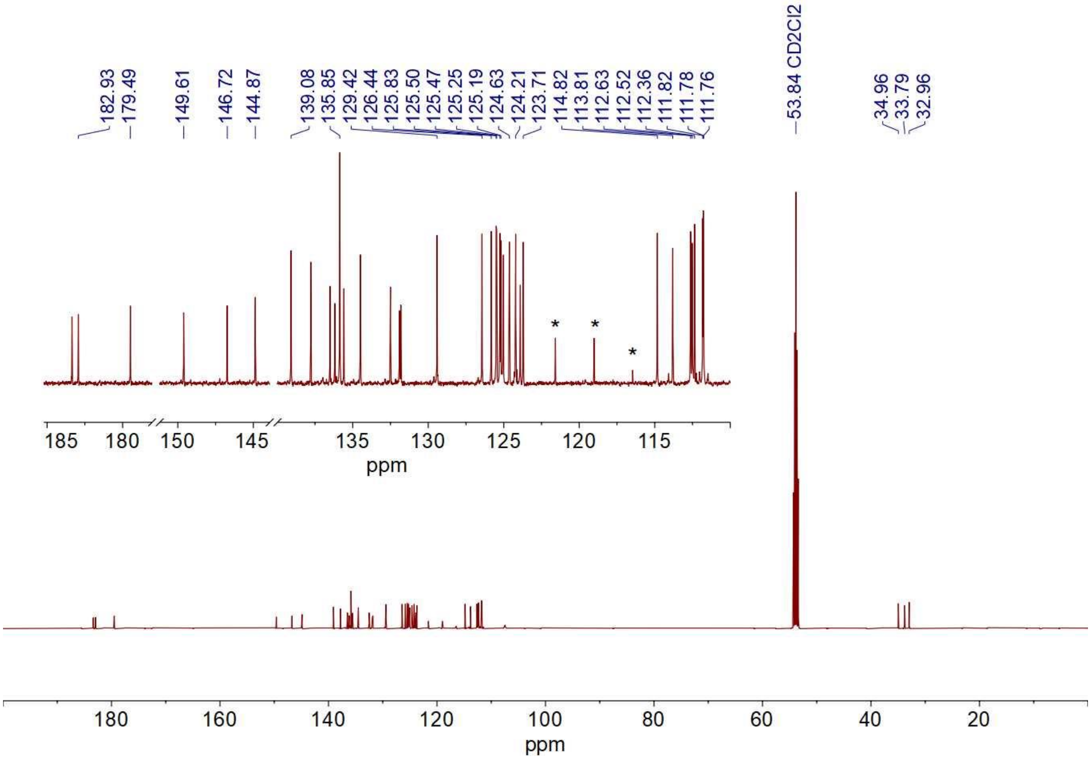

^{13}C NMR (126 MHz, CD_2Cl_2, 298 K) spectrum of [Ir(pmb)$_2$(Hpmb)](NTf$_2$). The signals of NTf$_2$ anion are marked by asterisks.

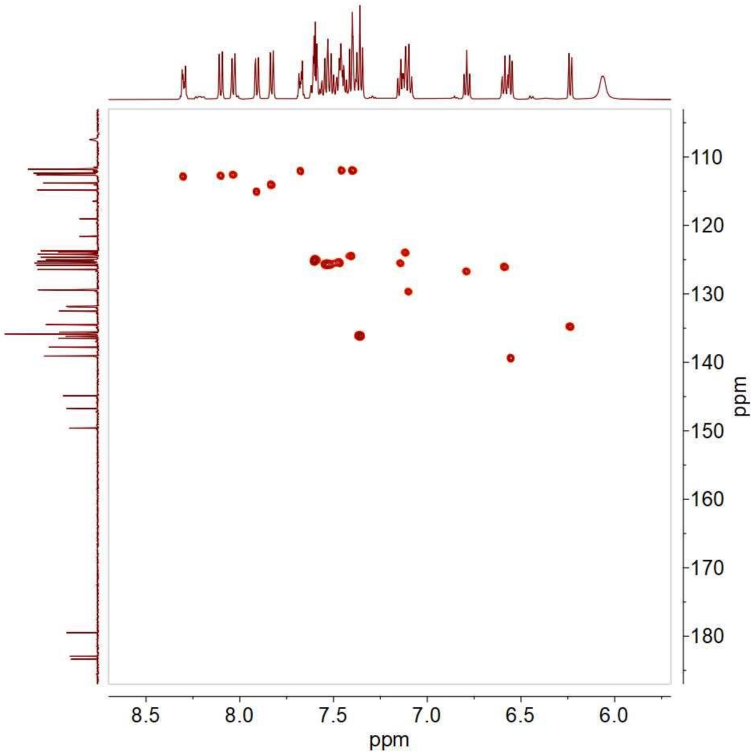

HSQC NMR (500 MHz, CD_2Cl_2, 298 K) spectrum of [Ir(pmb)$_2$(Hpmb)](NTf$_2$)

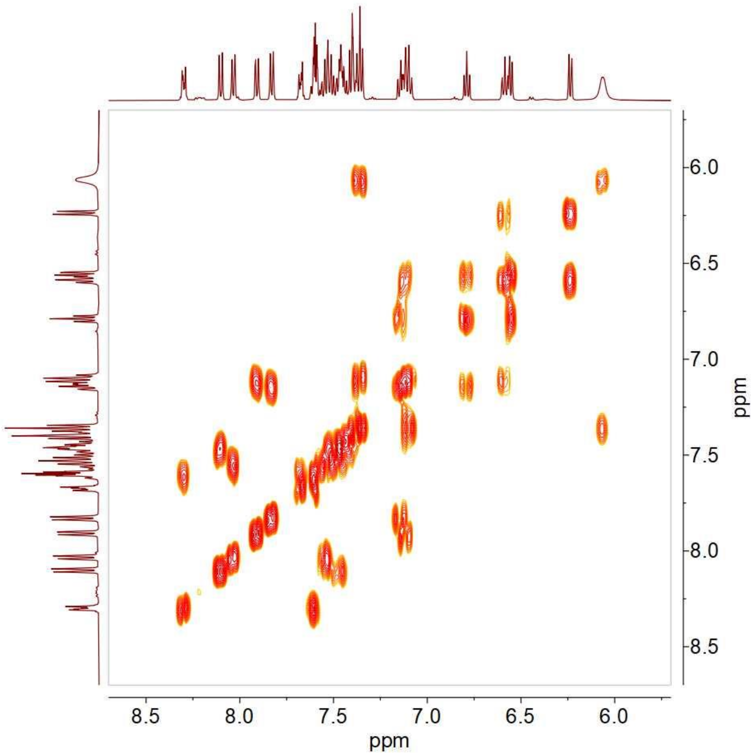

^{1}H–^{1}H COSY NMR (500 MHz, CD_2Cl_2, 298 K) spectrum of [Ir(pmb)$_2$(Hpmb)](NTf_2)

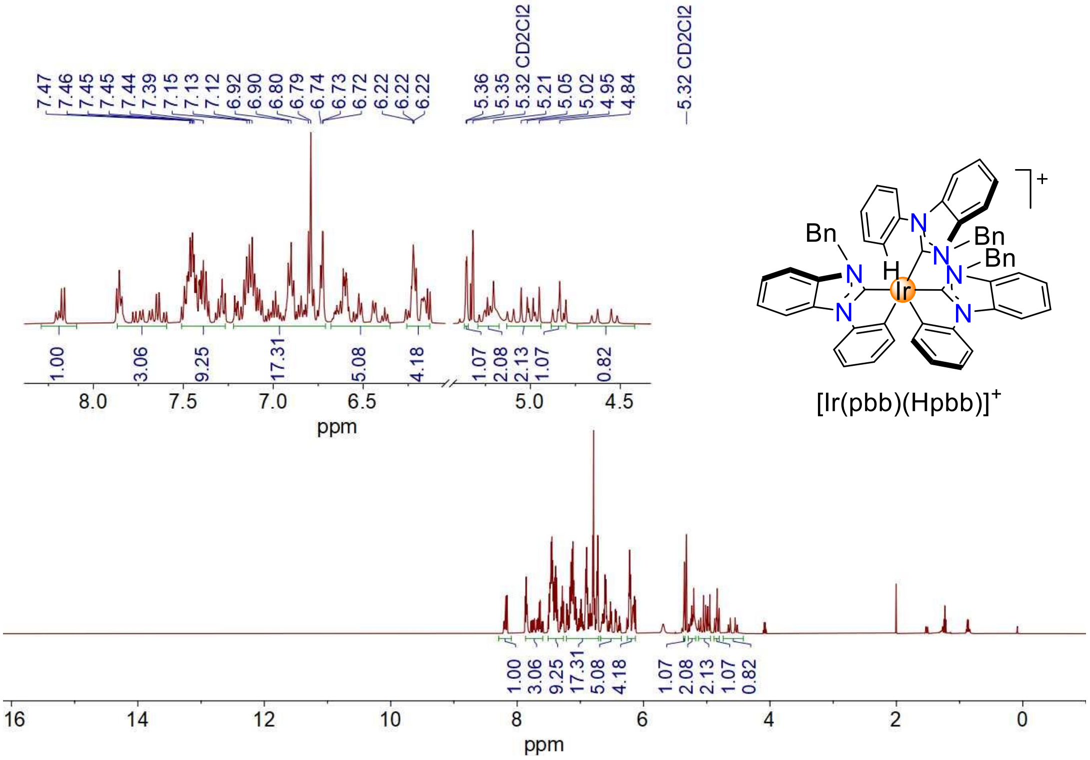

^{1}H NMR (500 MHz, CD_2Cl_2, 298 K) spectrum of [Ir(pbb)$_2$(Hpbb)](NTf_2). The NTf_2 anion is omitted for clarity.

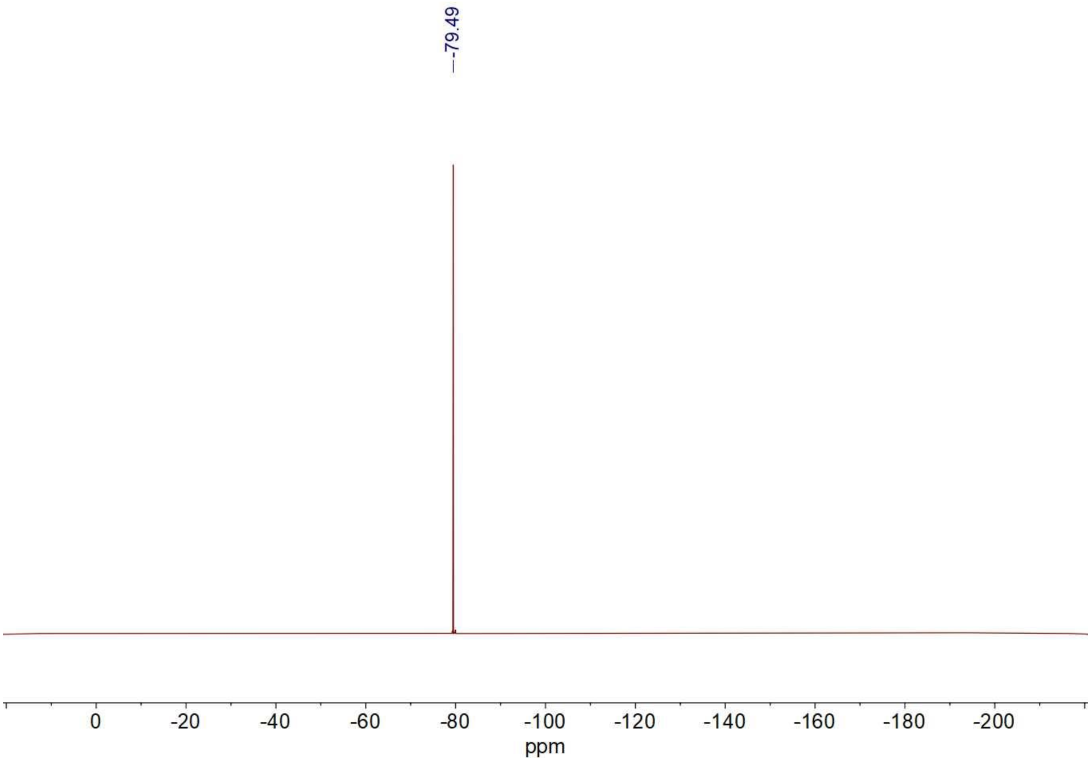

^{19}F NMR (376 MHz, CD_2Cl_2, 298 K) spectrum of [Ir(pbb)$_2$(Hpbb)](NTf_2)

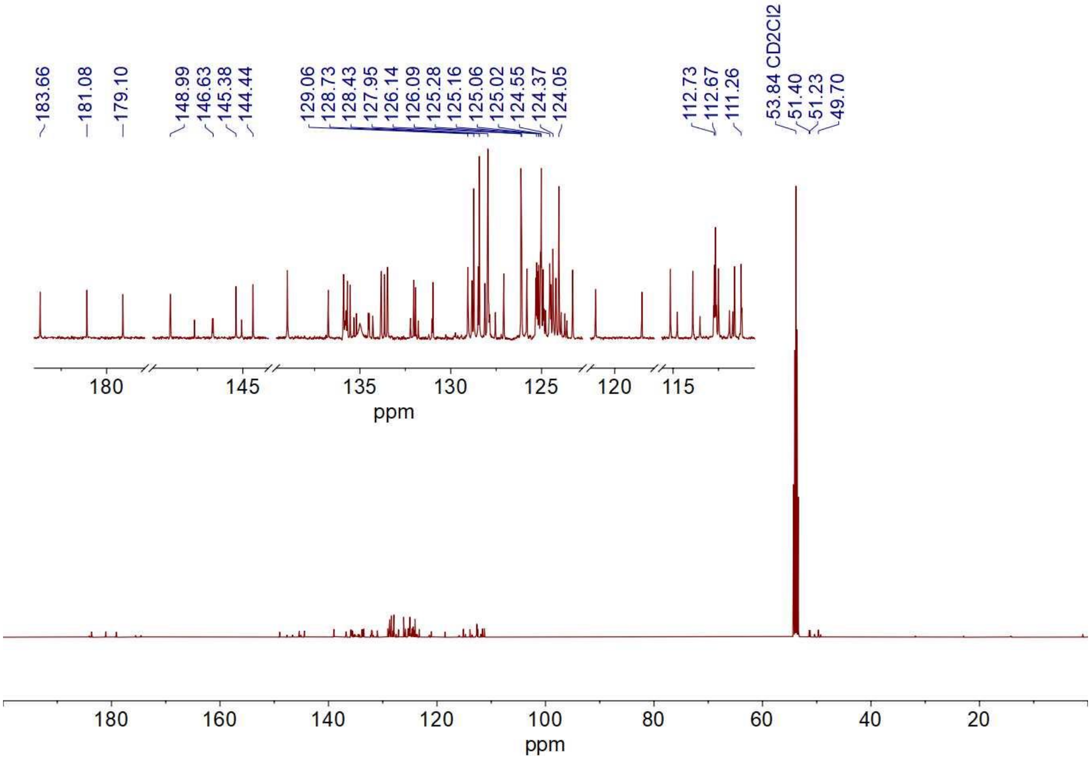

^{13}C NMR (126 MHz, CD_2Cl_2, 260 K) spectrum of [Ir(pbb)$_2$(Hpbb)](NTf_2)

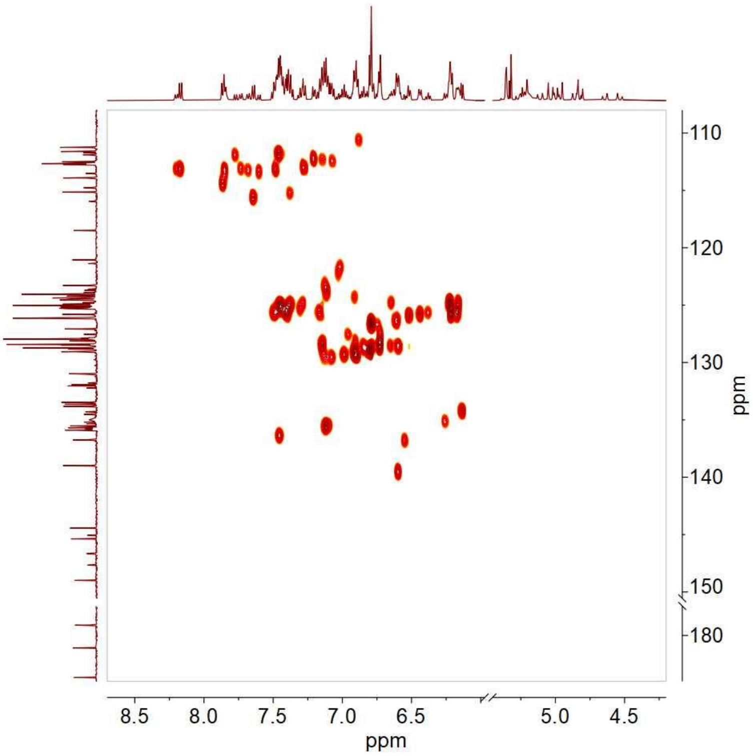

HSQC NMR (500 MHz, CD_2Cl_2, 260 K) spectrum of $[Ir(pbb)_2(Hpbb)](NTf_2)$

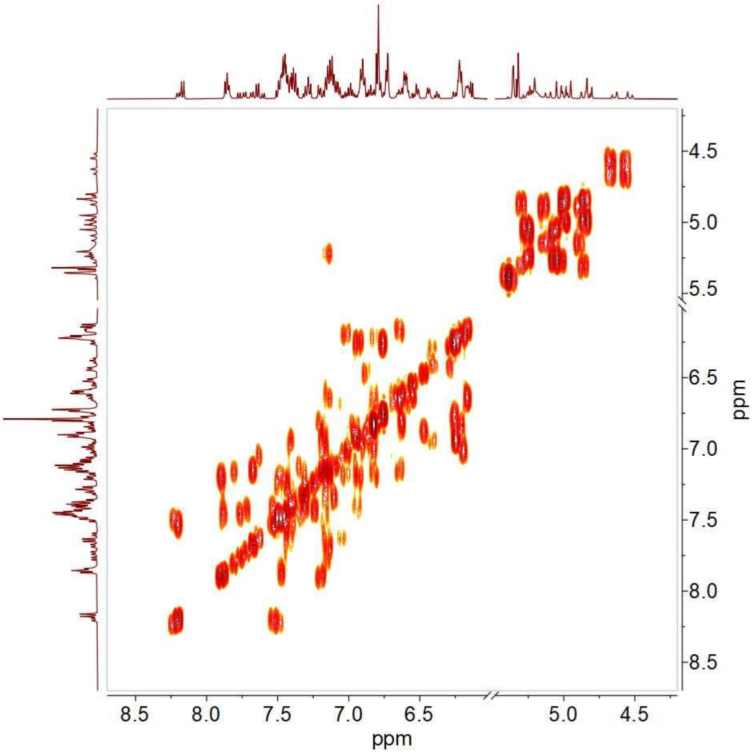

^1H–^1H COSY NMR (500 MHz, CD_2Cl_2, 298 K) spectrum of $[Ir(pbb)_2(Hpbb)](NTf_2)$

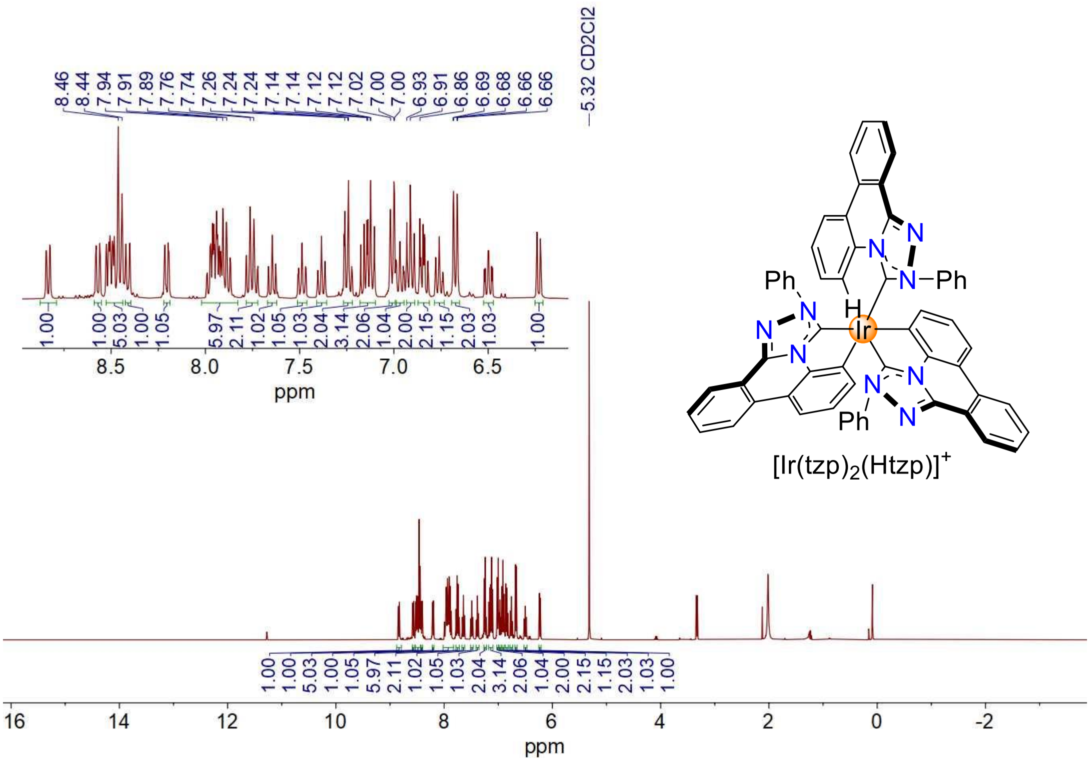

^{1}H NMR (500 MHz, CD_2Cl_2, 298 K) spectrum of [Ir(tzp)$_2$(Htzp)](NTf_2). The NTf_2 anion is omitted for clarity.

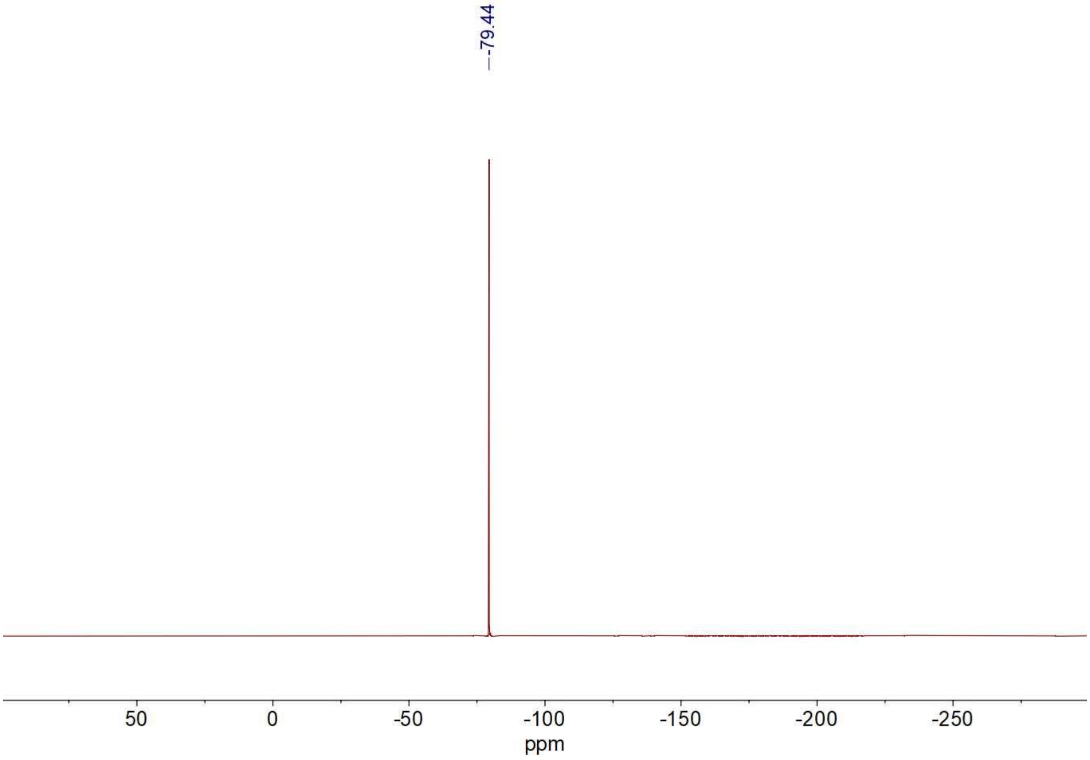

^{19}F NMR (376 MHz, CD_2Cl_2, 260 K) spectrum of [Ir(tzp)$_2$(Htzp)](NTf_2)

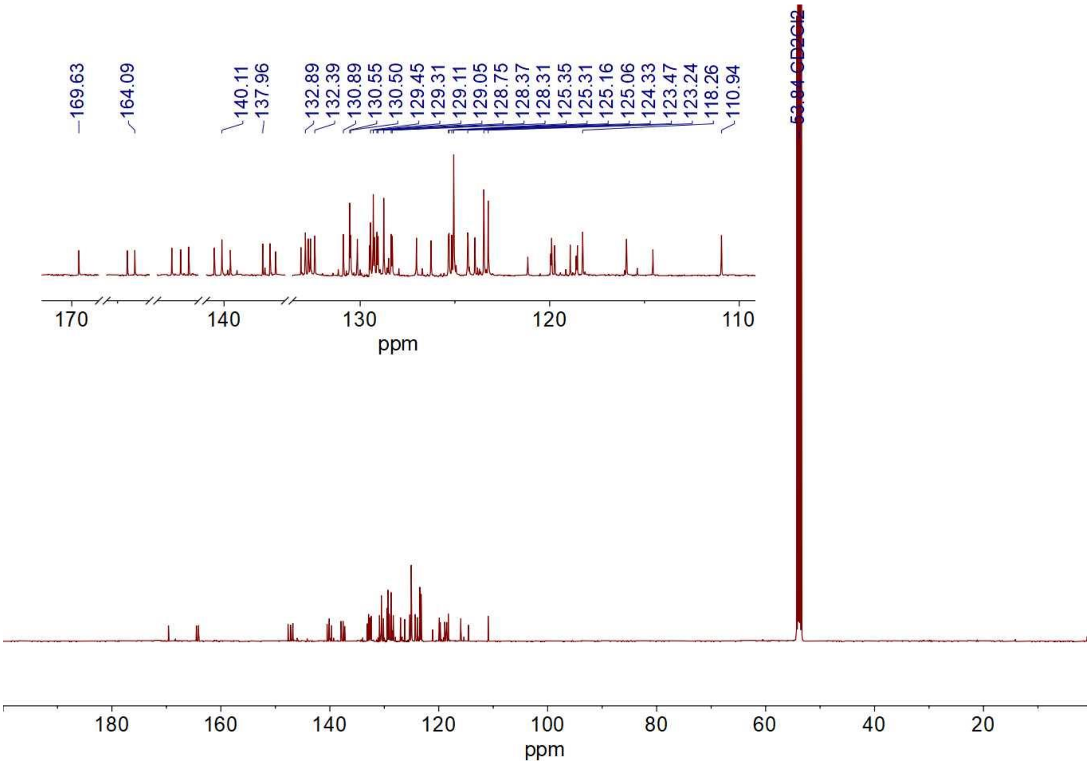

^{13}C NMR (126 MHz, CD_2Cl_2, 260 K) spectrum of $[Ir(tzp)_2(Htzp)](NTf_2)$

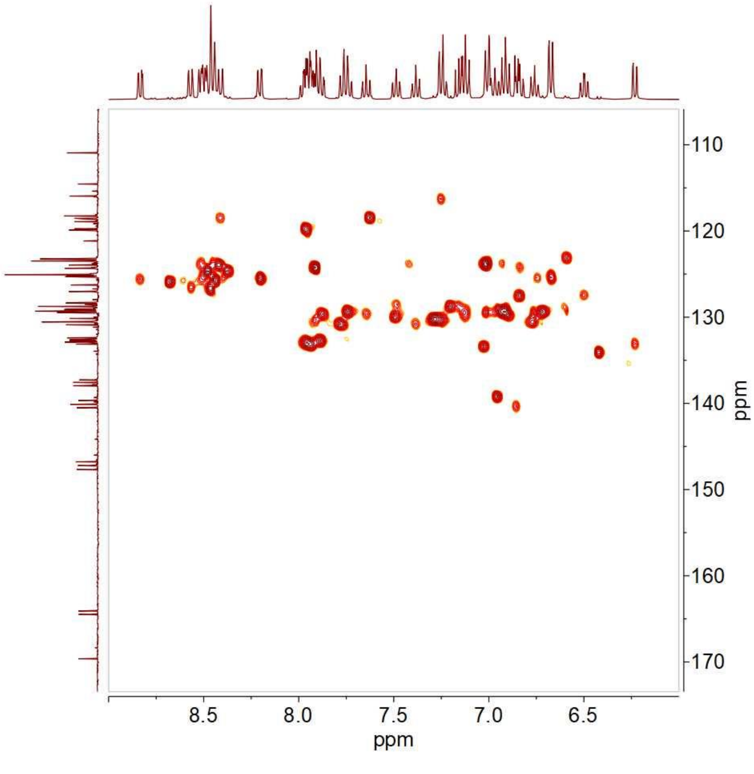

HSQC NMR (500 MHz, CD_2Cl_2, 260 K) spectrum of $[Ir(tzp)_2(Htzp)](NTf_2)$

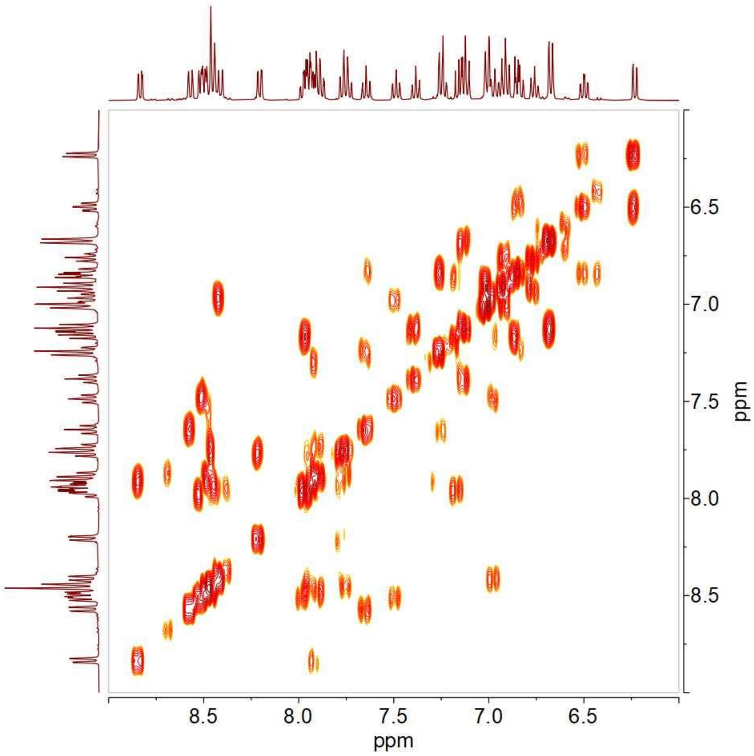

^{1}H–^{1}H COSY NMR (500 MHz, CD_2Cl_2, 298 K) spectrum of [Ir(tzp)$_2$(Htzp)](NTf_2)

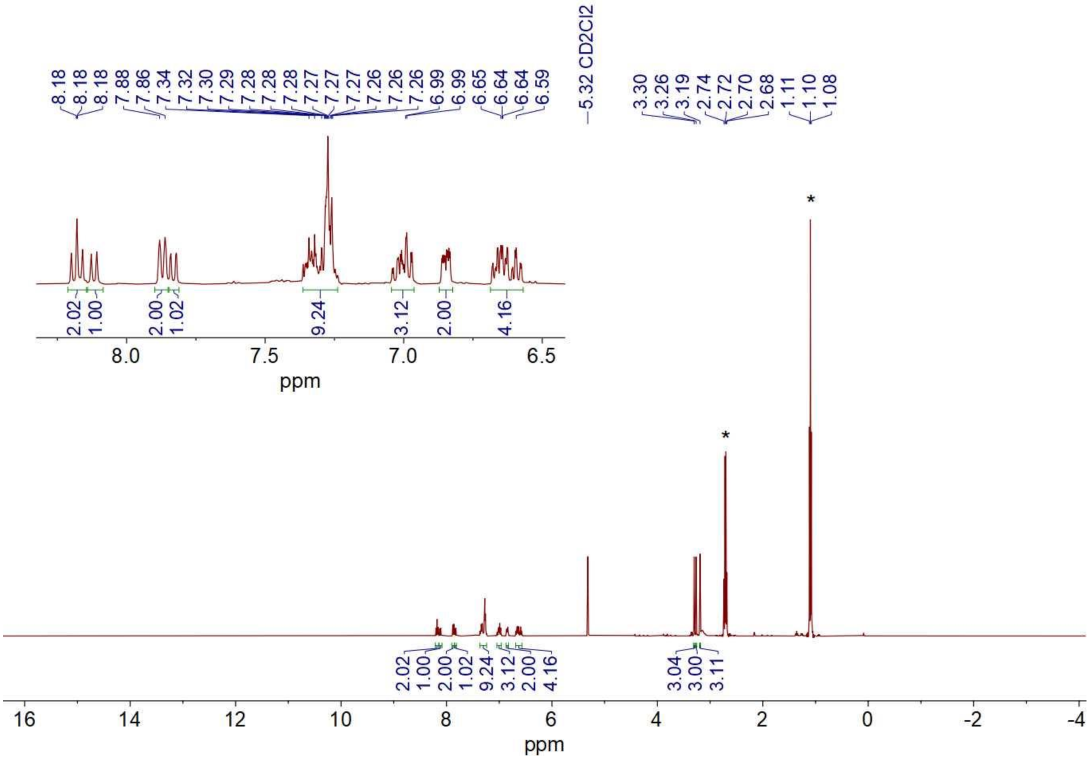

^{1}H NMR (400 MHz, CD_2Cl_2, 298 K) spectrum of *mer*-Ir(pmb)$_3$ obtained from *fac*-Ir(pmb)$_3$ by acid-base-induced *fac*→*mer* isomerization. The signals of ($NHEt_3$)(NTf_2) are marked by asterisks.

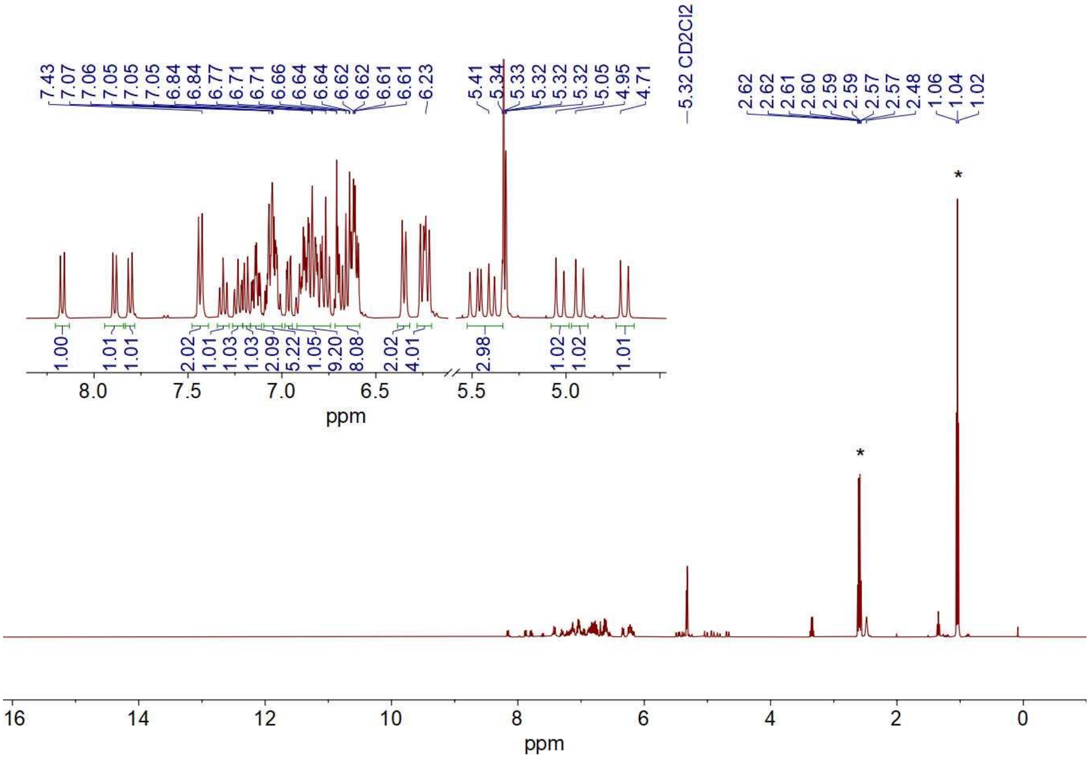

^{1}H NMR (400 MHz, CD_2Cl_2, 298 K) spectrum of *mer*-Ir(pbb)$_3$ obtained from *fac*-Ir(pbb)$_3$ by acid-base-induced *fac*→*mer* isomerization. The signals of $(NHEt_3)(NTf_2)$ are marked by asterisks.

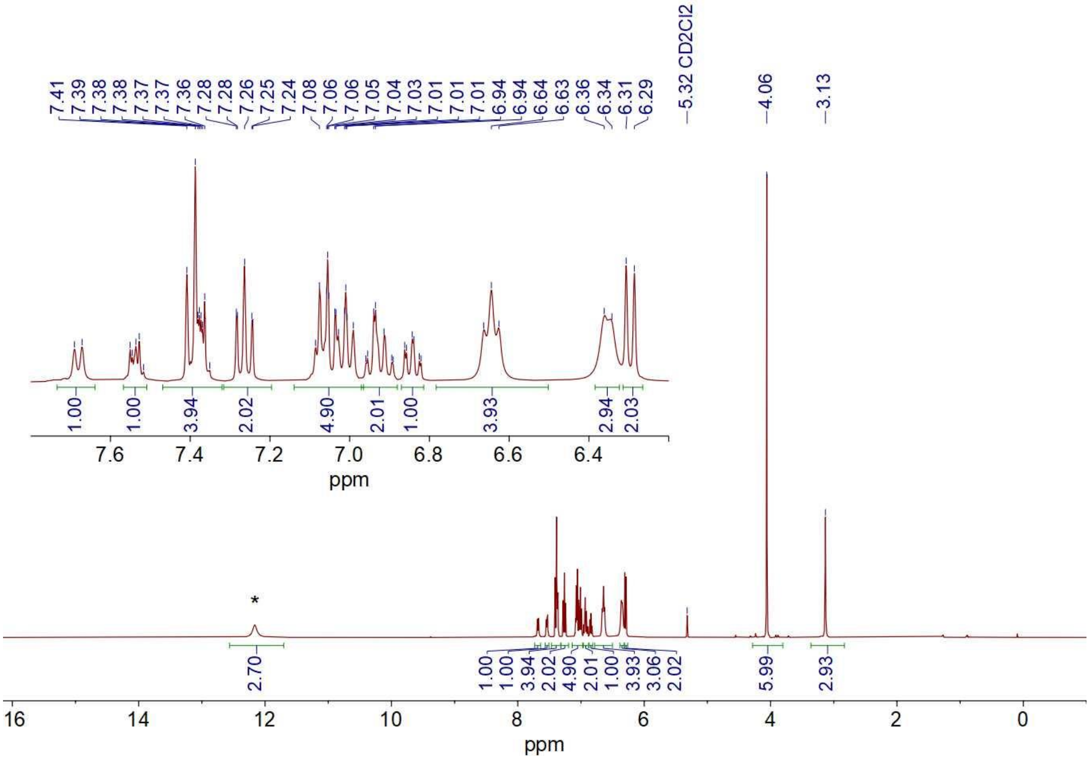

^{1}H NMR (400 MHz, CD_2Cl_2, 298 K) spectrum of [Ir(pmb)$_3$ + TFA]. The signal of TFA is marked by an asterisk.

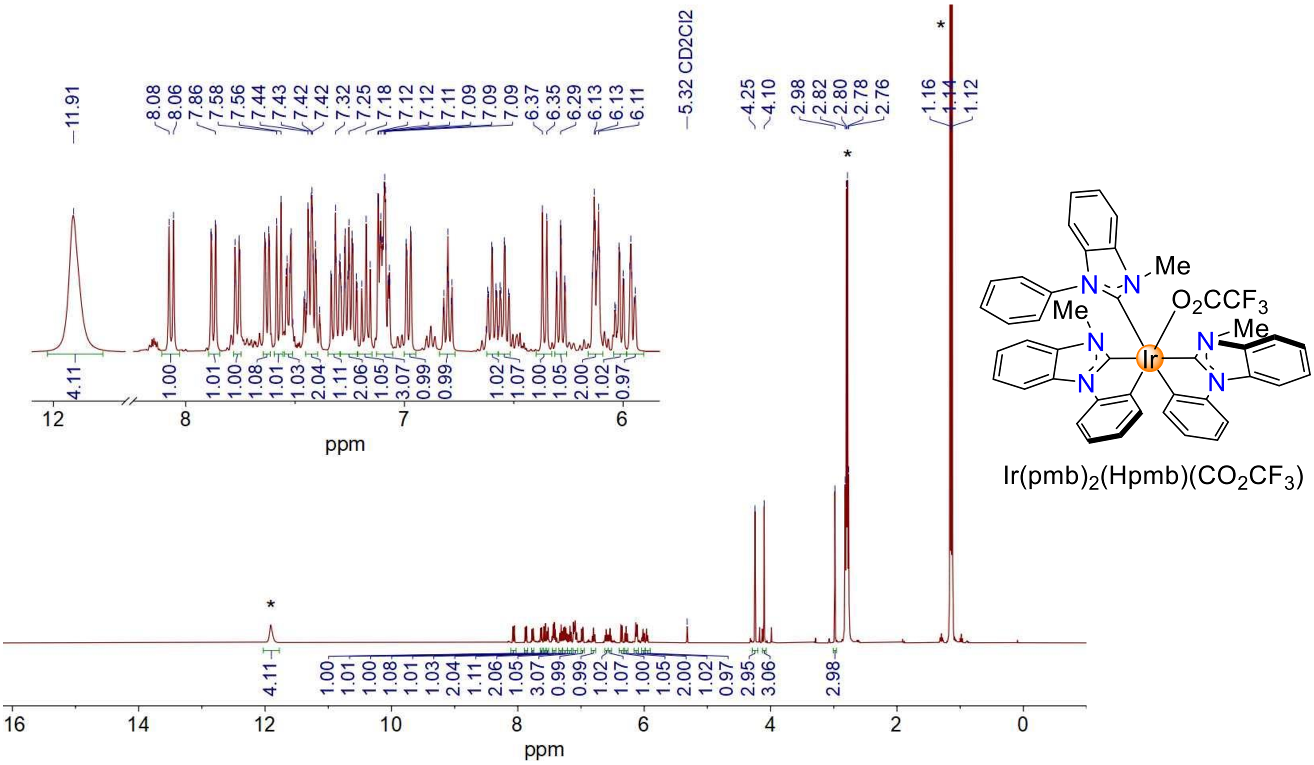

^{1}H NMR (400 MHz, CD_2Cl_2, 298 K) spectrum of Ir(pmb)(Hpmb)(CO_2CF_3). The signals of ($NHEt_3$)(CO_2CF_3) are marked by asterisks.

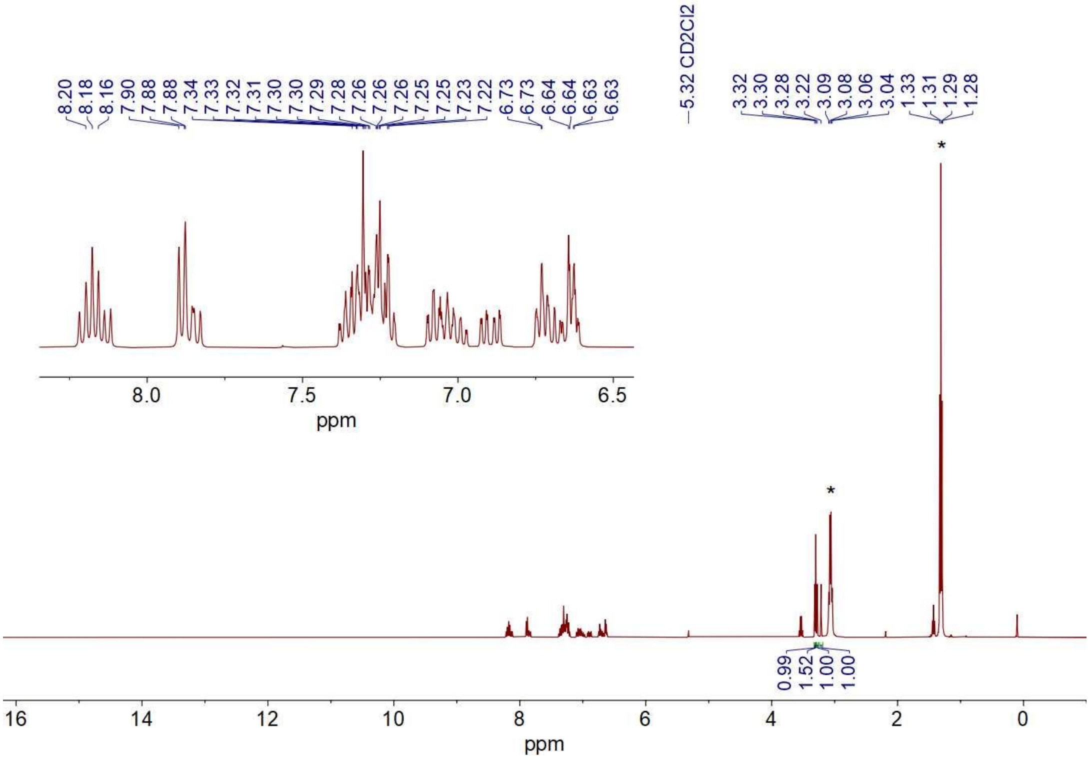

^{1}H NMR (400 MHz, CD_2Cl_2, 298 K) spectrum of the mixture of *fac*-Ir($pmb)_3$ and *mer*-Ir($pmb)_3$ obtained by the heating of Ir(pmb)(Hpmb)(CO_2CF_3) at 70 °C for 16 h. The signals of ($NHEt_3$)(CO_2CF_3) are marked by asterisks.

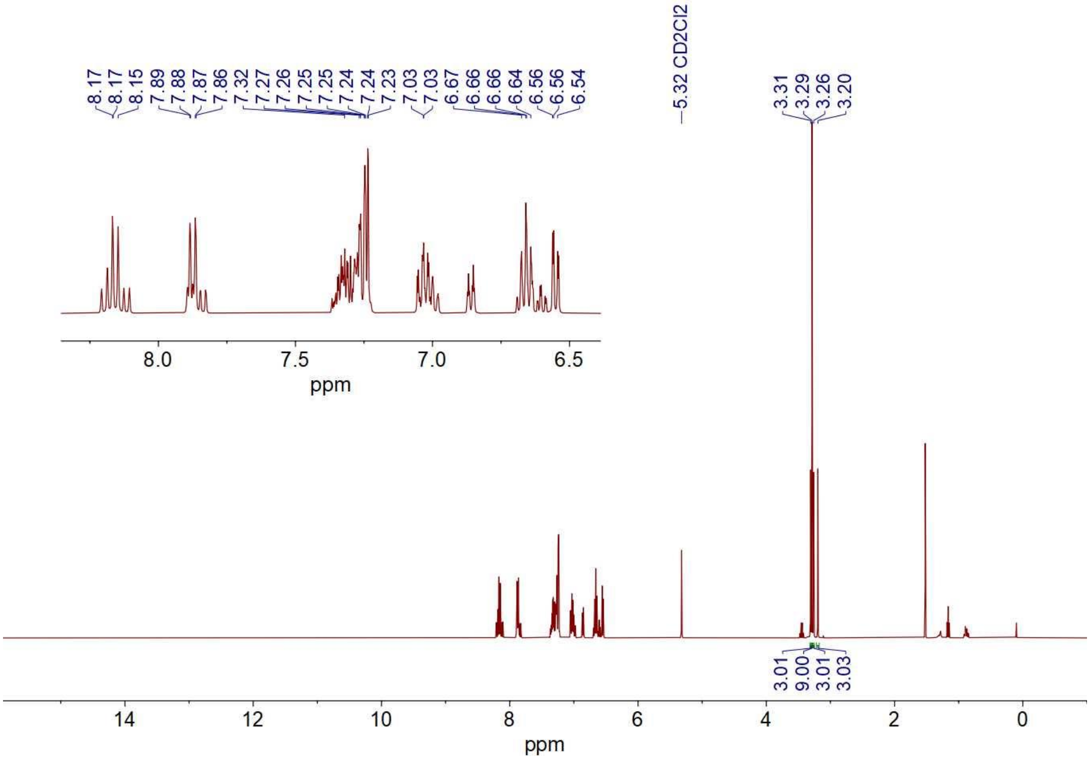

^{1}H NMR (400 MHz, CD_2Cl_2, 298 K) spectrum of the mixture *fac*-Ir(pmb)$_3$ and *mer*-Ir(pmb)$_3$ (1:1).

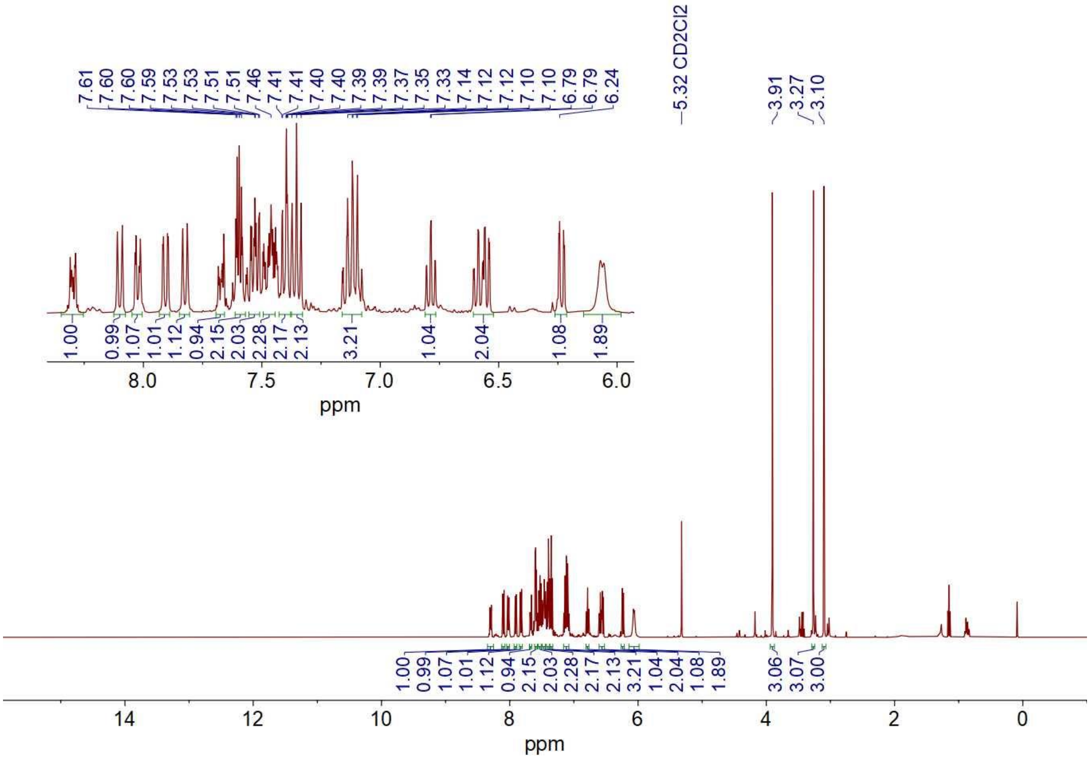

^{1}H NMR (400 MHz, CD_2Cl_2, 298 K) spectrum of [Ir(pmb)$_2$(Hpmb)](NTf$_2$) obtained by the treatment of the mixture *fac*-Ir(pmb)$_3$ and *mer*-Ir(pmb)$_3$ (1:1) with HNTf$_2$.

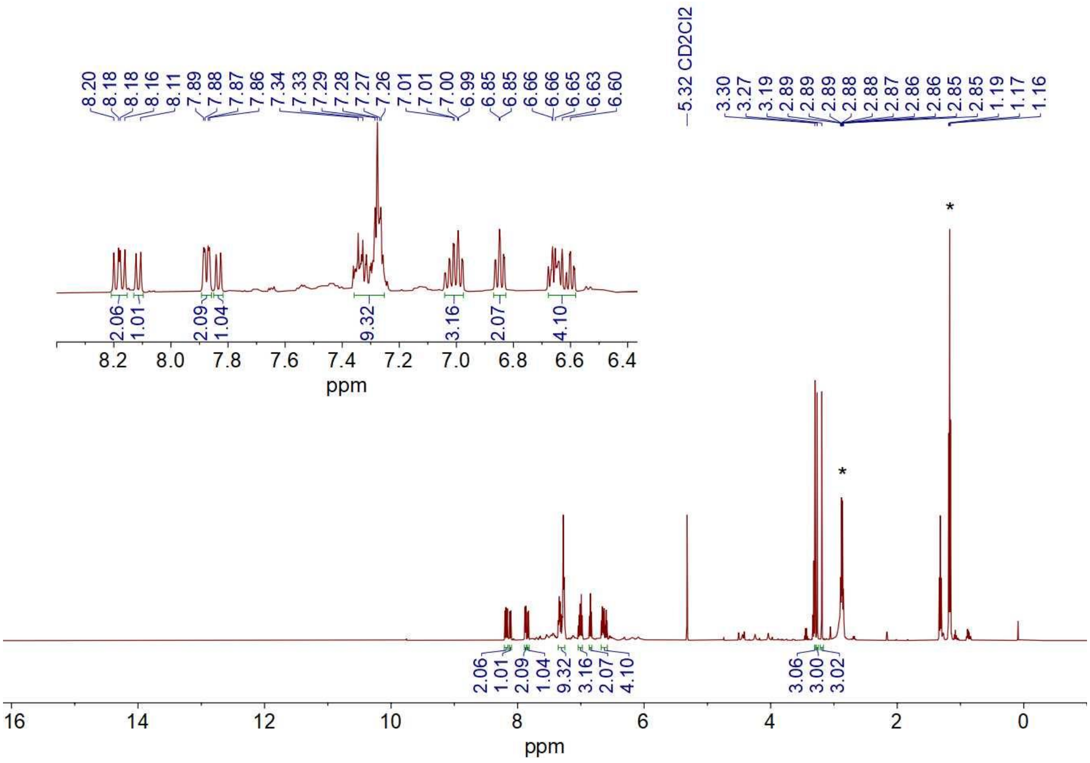

^{1}H NMR (400 MHz, CD_2Cl_2, 298 K) spectrum of *mer*-Ir(pmb)$_3$ obtained by the sequential treatment of the mixture *fac*-Ir(pmb)$_3$ and *mer*-Ir(pmb)$_3$ (1:1) by $HNTf_2$ and then NEt_3.

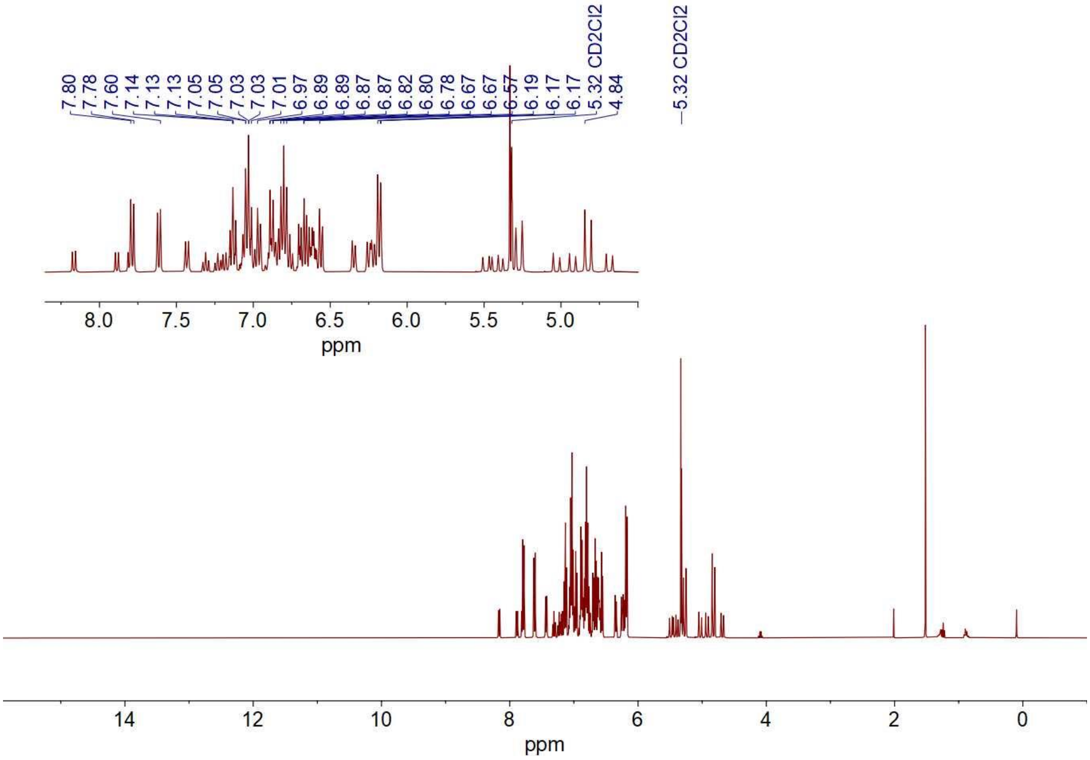

^{1}H NMR (400 MHz, CD_2Cl_2, 298 K) spectrum of the mixture *fac*-Ir(pbb)$_3$ and *mer*-Ir(pbb)$_3$ (1:1).

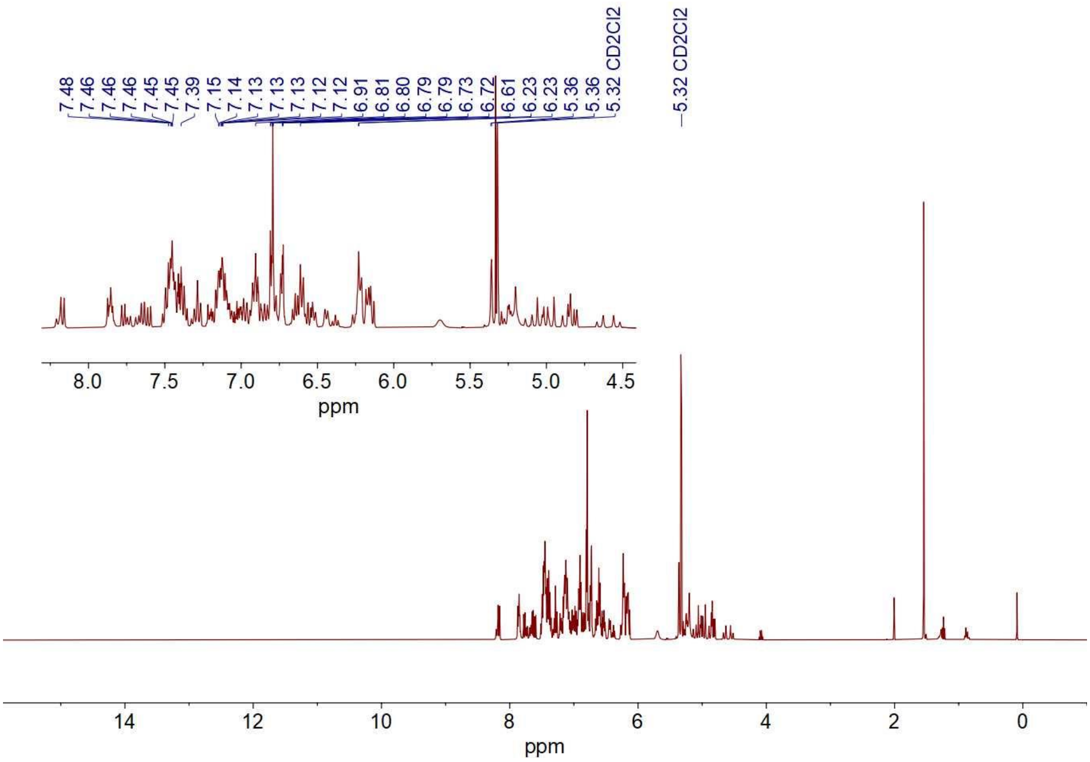

^{1}H NMR (400 MHz, CD_2Cl_2, 298 K) spectrum of [Ir(pbb)$_2$(Hpbb)](NTf_2) obtained by the treatment of the mixture *fac*-Ir(pbb)$_3$ and *mer*-Ir(pbb)$_3$ (1:1) with $HNTf_2$.

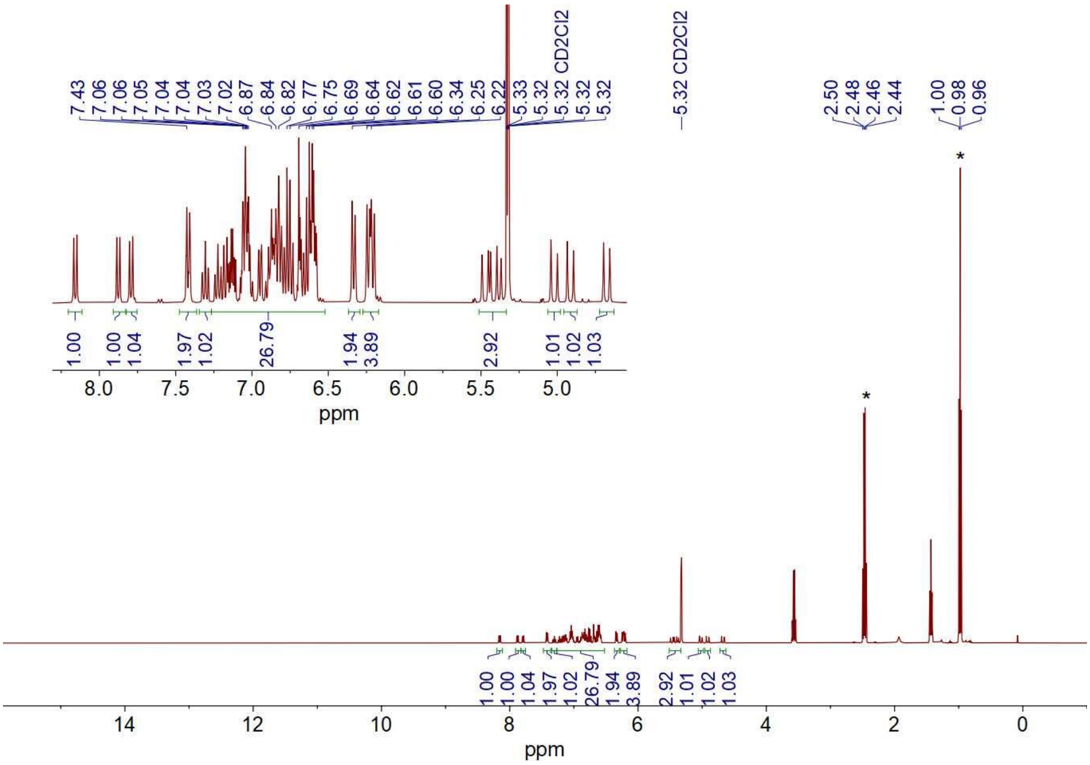

^{1}H NMR (400 MHz, CD_2Cl_2, 298 K) spectrum of *mer*-Ir(pbb)$_3$ obtained by the sequential treatment of the mixture *fac*-Ir(pbb)$_3$ and *mer*-Ir(pbb)$_3$ (1:1) by $HNTf_2$ and then NEt_3.

Mass spectra

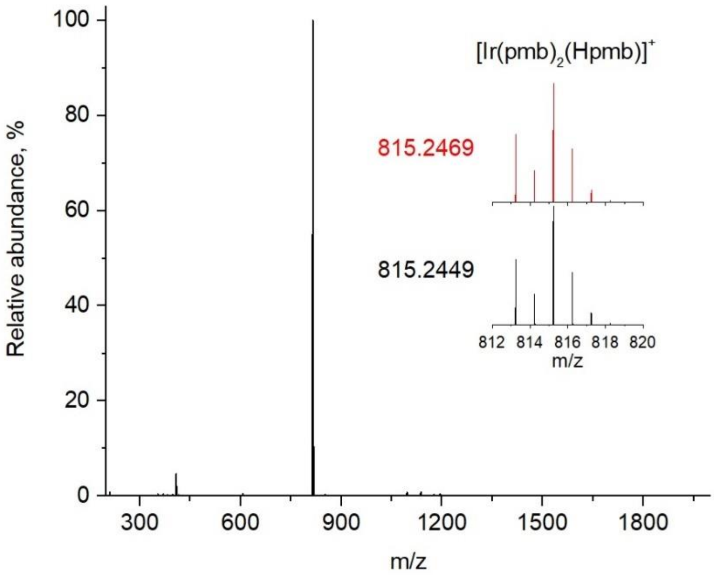

Nanochip-ESI⁺ HRMS of [Ir(pmb)$_2$(Hpmb)](NTf$_2$). The simulated spectrum is shown in red.

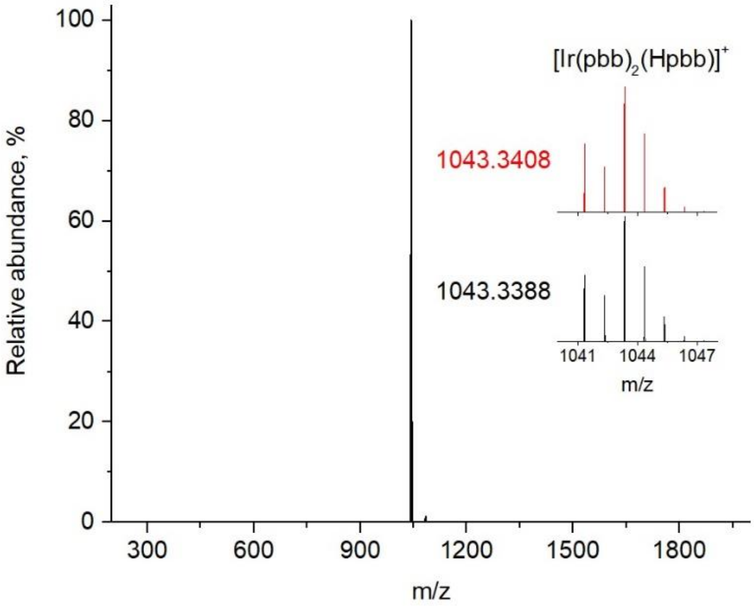

Nanochip-ESI⁺ HRMS of [Ir(pbb)$_2$(Hpbb)](NTf$_2$). The simulated spectrum is shown in red.

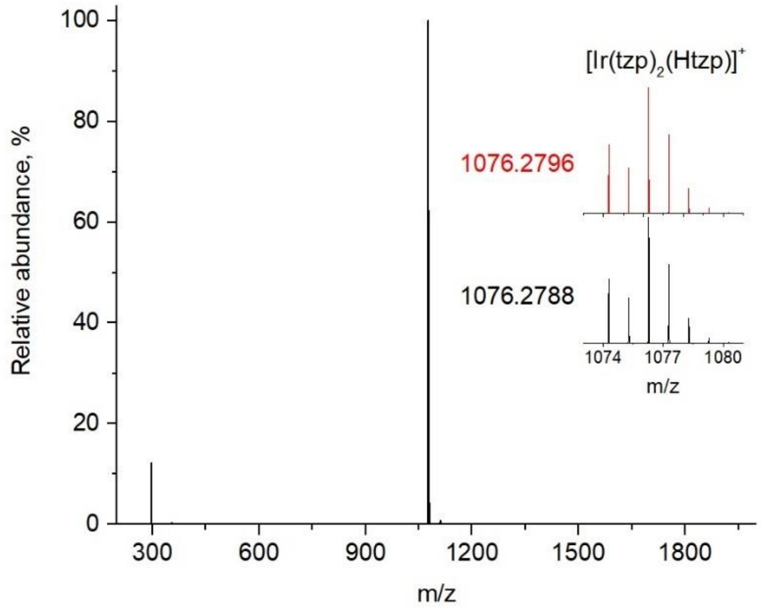

Nanochip-ESI$^+$ HRMS of [Ir(tzp)$_2$(Htzp)](NTf$_2$). The simulated spectrum is shown in red.

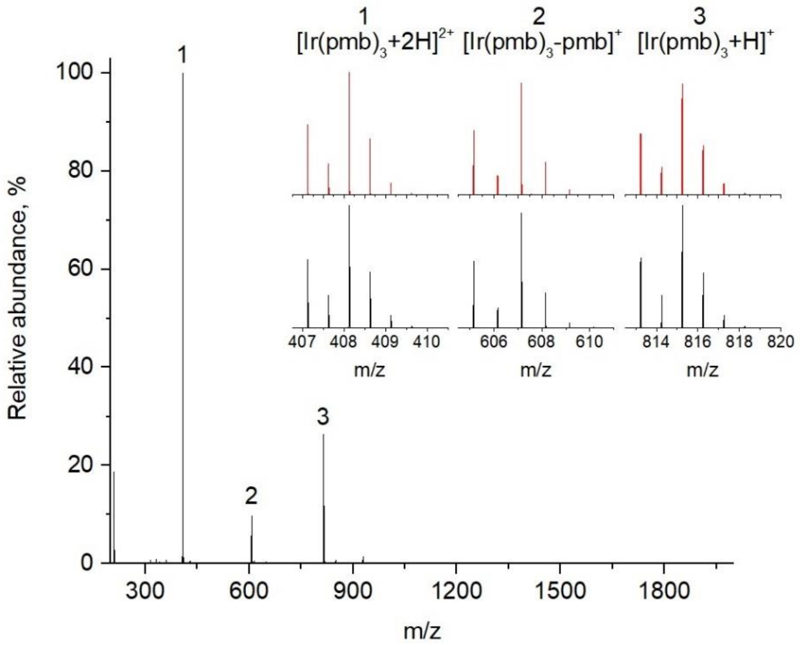

Nanochip-ESI$^+$ HRMS of the adduct of *fac*-Ir(pmb)$_3$ with TFA. Simulated spectra are shown in red.

References

1 G. R. Fulmer, A. J. M. Miller, N. H. Sherden, H. E. Gottlieb, A. Nudelman, B. M. Stoltz, J. E. Bercaw and K. I. Goldberg, *Organometallics*, 2010, **29**, 2176–2179.

2 J. G. Osiak, T. Setzer, P. G. Jones, C. Lennartz, A. Dreuw, W. Kowalsky and H. H. Johannes, *Chem. Commun.*, 2017, **53**, 3295–3298.

3 B.-S. Yun, S.-Y. Kim, J.-H. Kim, S. Choi, S. Lee, H.-J. Son and S. O. Kang, *ACS Appl. Electron. Mater.*, 2022, **4**, 2699–2710.

4 G. K. Sterligov, A. N. Lysenko, E. A. Drokin, L. I. Minaeva, M. A. Topchiy, A. A. Ageshina, S. A. Rzhevskiy, M. S. Nechaev and A. F. Asachenko, *Russ. Chem. Bull.*, 2022, **71**, 479–483.

5 CrysAlis^{Pro} Software System Rigaku Oxford Diffraction, 2022.

6 G. M. Sheldrick, *Acta Crystallogr. Sect. A*, 2015, **71**, 3–8.

7 G. M. Sheldrick, *Acta Crystallogr. Sect. C*, 2015, **71**, 3–8.